AWARD NUMBER: W81XWH-14-1-0502

TITLE: Smart Sensing and Dynamic Fitting for Enhanced Comfort and Performance of Prosthetics

PRINCIPAL INVESTIGATOR: Haiying Huang

CONTRACTING ORGANIZATION: University of Texas, Arlington
Arlington, TX 76019-0145

REPORT DATE: October 2016

TYPE OF REPORT: Annual

PREPARED FOR: U.S. Army Medical Research and Materiel Command
Fort Detrick, Maryland 21702-5012

REPORT DOCUMENTATION PAGE

Form Approved
OMB No. 0704-0188

1. REPORT DATE	**2. REPORT TYPE**	**3. DATES COVERED**
October 2016	Annual	30Sep2015 - 29Sep2016

4. TITLE AND SUBTITLE

Smart Sensing and Dynamic Fitting for Enhanced Comfort and Performance of Prosthetics

5a. CONTRACT NUMBER

5b. GRANT NUMBER
W81XWH-14-1-0502

5c. PROGRAM ELEMENT NUMBER

6. AUTHOR(S)

Haiying Huang

E-Mail: huang@uta.edu

5d. PROJECT NUMBER

5e. TASK NUMBER

5f. WORK UNIT NUMBER

7. PERFORMING ORGANIZATION NAME(S) AND ADDRESS(ES)

University of Texas Arlington
500 W. First Street, WH211
Arlington, TX 76019

8. PERFORMING ORGANIZATION REPORT NUMBER

9. SPONSORING / MONITORING AGENCY NAME(S) AND ADDRESS(ES)

U.S. Army Medical Research and Materiel Command
Fort Detrick, Maryland 21702-5012

10. SPONSOR/MONITOR'S ACRONYM(S)

11. SPONSOR/MONITOR'S REPORT NUMBER(S)

12. DISTRIBUTION / AVAILABILITY STATEMENT

Approved for Public Release; Distribution Unlimited

13. SUPPLEMENTARY NOTES

14. ABSTRACT

The objective of the project is to enhance the long-term fit and performance of prosthetic sockets through smart sensing, adaptive interface, and shear-based dynamic fitting strategy. In the second year, the sensor development effort has been focused on 1) fabricating custom-made prosthetic liners with the sensors embedded and 2) developing a portable dynamic sensor interrogation unit. We have implemented a test fixture for sensor characterization and validated that the shear/pressure sensor fabricated in soft liner material has an uncertainties of around +/-10% of the full range. A portable interrogator was developed to achieve dynamic sensor interrogation at a sampling rate of 200 Hz. For actuation, we have characterized the load bearing capability of air cell actuator arrays at different actuation pressures. A "limb-socket" laboratory test setup was developed for capturing the internal pressure change of air cell actuators when the "limb" was subjected to the external force.

15. SUBJECT TERMS

Prosthetic socket, interface, shear/pressure sensor, antenna sensor, active interface, actuator inserts, PTBAFO, Control System, Graphic User Interface (GUI), microprocessor

16. SECURITY CLASSIFICATION OF:			**17. LIMITATION OF ABSTRACT**	**18. NUMBER OF PAGES**	**19a. NAME OF RESPONSIBLE PERSON**
a. REPORT	**b. ABSTRACT**	**c. THIS PAGE**			USAMRMC
Unclassified	Unclassified	Unclassified	Unclassified	34	**19b. TELEPHONE NUMBER** *(include area code)*

Contents

1 Introduction 2
2 Keywords 2
3 Accomplishments 2
4 Impact 19
5 Changes/Problems 20
6 Products 20
7 Participants & Other Collaborating Organizations 21
8 Special Reporting Requirements 22
9 Appendices 22

1 INTRODUCTION

The objective of the project is to enhance the long-term fit and performance of prosthetic sockets through smart sensing, adaptive interface, and shear-based dynamic fitting strategy. In the second year, the sensor development effort has been focused on 1) fabricating custom-made prosthetic liners with the sensors embedded and 2) developing a portable dynamic sensor interrogation unit. We have implemented a test fixture for sensor characterization and validated that the shear/pressure sensor fabricated in soft liner material has an uncertainties of around $\pm$10% of the full range. A portable interrogator was developed to achieve dynamic sensor interrogation at a sampling rate of 200 Hz. For actuation, we have characterized the load bearing capability of air cell actuator arrays at different actuation pressures. A "limb-socket" laboratory test setup was developed for capturing the internal pressure change of air cell actuators when the "limb" was subjected to the external force.

2 KEYWORDS

Prosthetic socket, interface, shear/pressure sensor, antenna sensor, active interface, actuator inserts, PTB-AFO, Control System, Graphic User Interface (GUI), microprocessor

3 ACCOMPLISHMENTS

- **What were the major goals of the project?**

The three aims of the projects are: 1) Demonstrating real-time measurements of interfacial stresses and residual limb volume; 2) Producing active interfaces that can automatically adjust the fitting of the prosthetic socket; 3) Testing the active prosthetic interface and the shear-based fitting strategy in clinical settings.

First year milestones:

- *Milestone #1: Author manuscript that demonstrates simultaneous measurement of shear and pressure stresses (by July 2015) – experiment is completed. Manuscript preparation under way.*
- *Milestone #2:Author manuscript that demonstrates volume and bio-impedance sensing using antenna sensors (postponed to focused on implementing antenna shear/pressure sensor in custom prosthetic liner)*
- *(Added) Demonstrate sensor implementation in custom made prosthetic liner - completed*
- *Milestone #4:Demonstrate a laboratory prototype that can dynamically change pressure profile (by September 2015) –completed*

Second year milestones:

- *Milestone #5:Demonstrate an active fitting system for subtask 5 (by October 2016) -75% completed*
- *Milestone #7: HRPO** approval received (IRB approved by UTSW, HRPO under review at CDMRP)*

- **What was accomplished under these goals?**

*Accomplishment #1***:** validated the shear and pressure sensing capabilities of antenna sensor embedded in soft silicon material

- **Specific objective:** develop test fixture that can be used for the characterization of soft material and soft antenna sensor
- **Major activities**:

1) Develop test fixture for soft material and sensor characterization: to enable detailed characterizations of soft materials, a cantilever beam load cell was design to be integrated with the test fixture. As shown in figure 1(a), the cantilever beam has a slot at the center so that the strain gauges bonded on the outer walls of the slot have sufficient sensitivity to measure small compression and bending load changes. A plastic plate attached to the bottom of the cantilever beam enables applying shear and pressure to the soft material while the top of the cantilever beam is fixed to the movable shear plate. This test fixture was used for (i) characterizing the material properties of silicone materials, as shown

in figure 1(a); and (ii) performing shear and compression tests of the antenna sensors embedded in liner materials (see figure 1(b)). An Arduino Mega shield was developed to house the circuits for signal conditioning, motor control, and pressure regulation, as shown in figure 1(c). A Excel visual basic program was developed to control pressure and shear application and to acquire the sensor data automatically. Automation of the test fixture enables performing the test in a timely fashion.

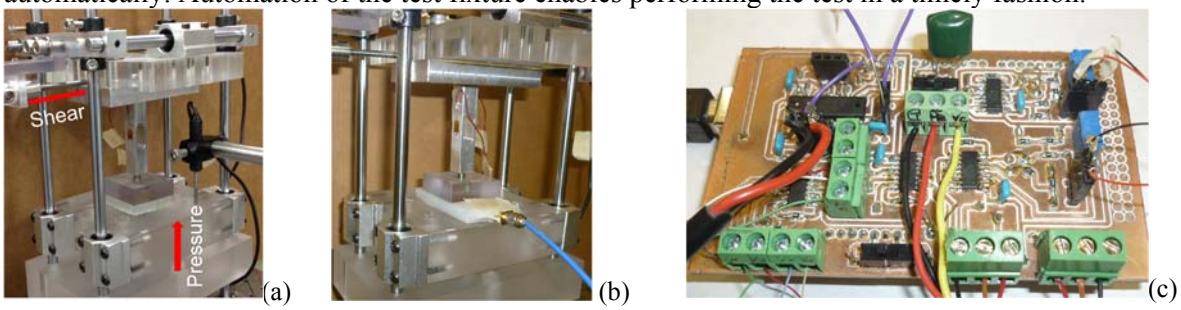

(a) (b) (c)

Figure 1: a test fixture a cantilever beam load cell for (a) testing the shear and pressure moduli of soft silicon material; (b) characterizing the shear and pressure sensing capability of the soft antenna sensor; (c) Arduino mega–based control unit for automation of the test fixture.

2) Test the compression and shear moduli of soft materials: different silicone materials were used to fabricate 41x41 mm^2 cubes with a thickness of 5-6 mm. These cubes were tested in three different test conditions: a) under pressure only; (b) under shear displacements and a constant pressure of 13 psi; and (c) under shear displacements and a constant pressure of 18 psi. The displacement-pressure relationships of various materials are compared with that of prosthetic linear material in figure 2(a). The slope of each curve corresponds to the compression modulus, i.e. the Young's modulus, of the material. Similarly, the displacement-shear force relationships of various silicone materials are compared with that of the liner material in figure 2(b). The slope of the curve corresponds to the shear modulus of the material. Based on these two figures, we found that the fabric laminated on the commercial liner alters the material properties of the prosthetic liner material significantly. Therefore, the selection of the silicone material was based on the material properties of the liner material with the fabric removed.

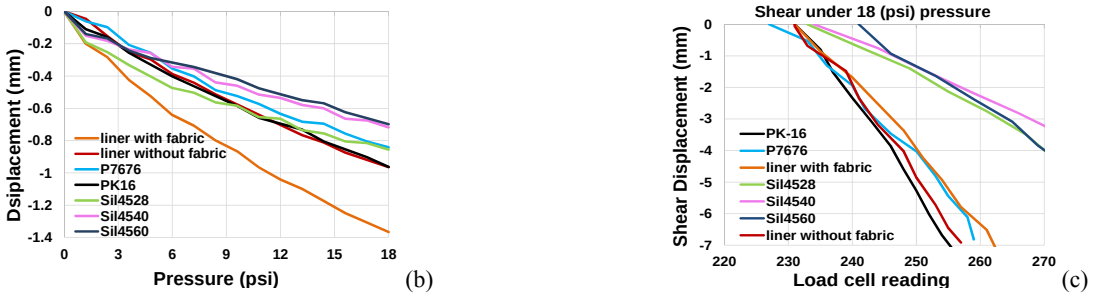

(b) (c)

Figure 2: characterize the compression and shear moduli of silicone materials; (a) comparison of displacement-pressure relationships of different materials; (b) comparison of displacement-shear load relationship of different materials.

- **Significant results:**

1) Selected silicone material for custom made prosthetic liner: based on the figures shown in figure 2, the materials with slopes similar to that of the prosthetic liner were classified into the two groups; materials P7676 and PK16 from Wacker and materials Sil4528, Sil4540 and Sil4560 from Silbione. This material property data help us to reduce the trial and error of embedding the antenna sensor in

different silicone materials. PK16 was selected for sensor and linear fabrication because it has greater tear resistance and tensile strength due to additional cross-linking of the polymer chains. However, this material can only be purchased in a large volume. Two materials from Smooth-on was found to have similar properties as PK16. We are currently evaluating the sensor performance fabricated on these two materials.

2) Characterized antenna sensor embedded in silicone material: the resonant frequencies of the antenna sensor embedded in the silicone material under different shear and compression displacements are shown in figure 3(a) and 3(b). They were fitted with second order polynomials and have an R-square value of 0.9986 and 0.9832, respectively. Based on these fitting equations, the applied shear and pressure were inversely determined from the antenna resonant frequencies. As shown in figure 3(c) and 3(d), the measurement uncertainties for both shear and pressure are around +/- 10% of the full range.

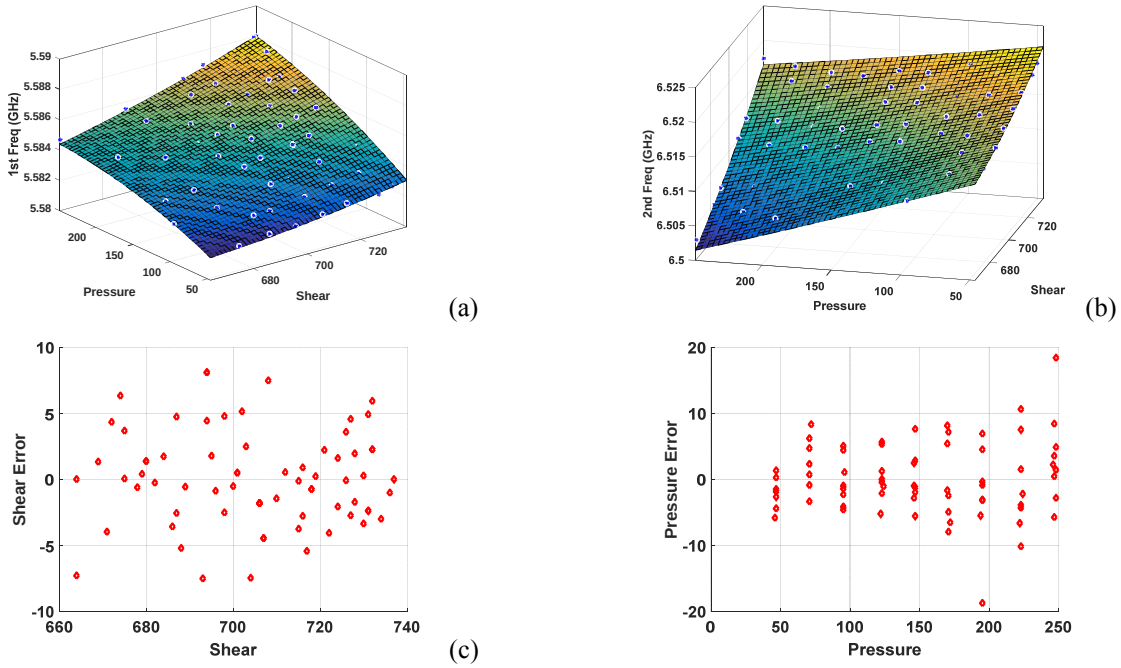

Figure 3: Performance of antenna sensor embedded in soft silicone material; (a) and (b) antenna resonant frequencies under different shear and pressure combination. The measurement data fit well with second-order polynomial functions; (c) and (d) errors between the applied shear and pressure and the actual inputs.

3) Validated the performance of the cantilever beam load cell: the cantilever beam load cell was calibrated under pure compression and combined shear/pressure loads. As shown in figure 4, the two strain gauges had almost identical performance under pure compression while they had opposite behavior under combined shear/pressure loading. By validating the performance of the cantilever beam load cell, we can install cantilever beam load cells on prosthetic liners to calibrate the antenna sensor embedded in prosthetic liners.

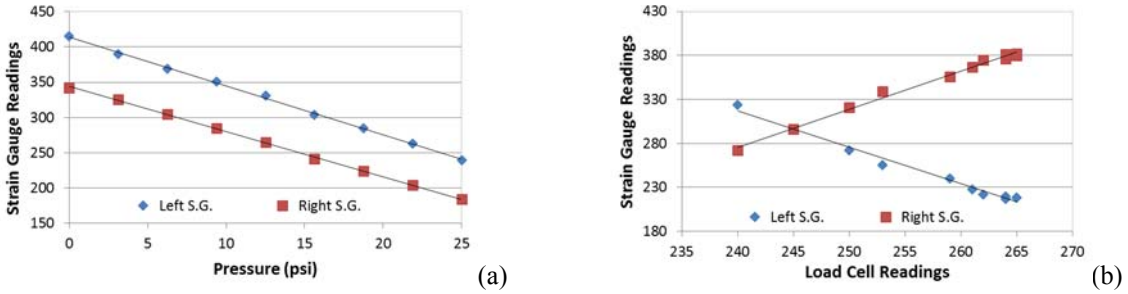

(a) (b)

Figure 4: Validation of cantilever beam load cell; (a) strain gauge readings under pure compression; (b) strain gauge readings under combined shear and compression.

Accomplishment #2: fabricated custom prosthetic liner embedded with antenna shear/pressure sensor

- **Specific objective:** develop design and fabrication techniques to embed the antenna sensor in prosthetic liners
- **Major activities**:

1) Design and fabricate antenna sensors with a long transmission line: in order to place the antenna sensor at the desired locations of the prosthetic liner, the antenna sensor should be fed with a transmission line of sufficient length. Typically, an antenna sensor is fed using a uniform 50 □ transmission line. Due to the thin substrate, however, the width of a 50 □ transmission line is only 0.32 mm, which makes fabrication difficult. To increase the width of the transmission line, we used quarter-wavelength matching to match the antenna impedance to a lower impedance and thus allows for a wider transmission line. The simulation model of the new antenna design, built using an EM simulation tool, Sonnet pro, is shown in figure 5(a). The input impedance of the patch at the edge was found to be 70 □. This impedance is transformed to an impedance of 10 Ω using a quarter-wave transformer, which corresponds to a transmission line width of 1.8 mm. At the connector end, the impedance of the transmission line is again transformed by a quarter-wave transformer to match the 50 Ω impedance of the SMA connector. The fabricated antenna sensor is shown in figure 5(b).

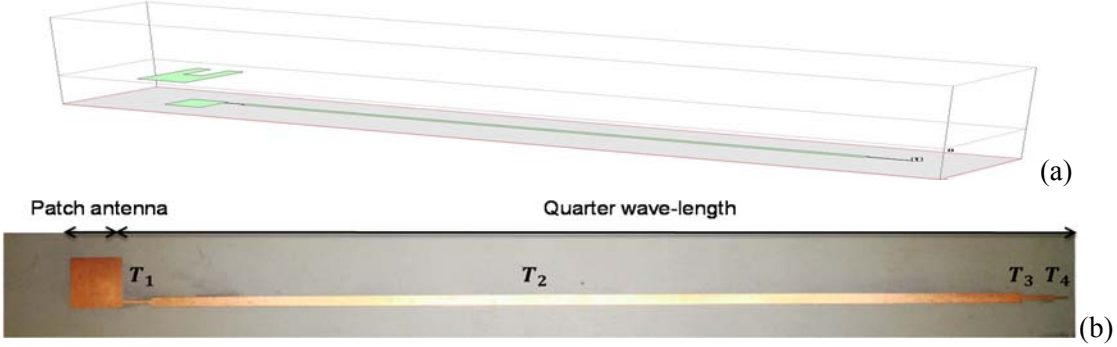

(a) (b)

Figure 5: Antenna sensors with a long transmission line; (a) numerical simulation model of shear/ pressure antenna sensor with two quarter-wavelength transformers; (b) patch antenna and transmission line fabricated on soft substrate.

2) Develop data processing algorithm to the S11 parameter measured from the antenna with a long transmission line: the S11 parameter measured from the antenna with a long transmission line has many valleys instead of two dominate valleys as predicted by the simulation (see figure 6(a)). In order to identify the cause of these additional valleys, the frequency-domain S11 parameter is converted to time-domain signal shown in figure 6(b). The time-domain signal at time "0" is due to the reflection at the connector while the signal in red are the reflection from the antenna sensor. Due to the long transmission line, these two reflections generate interference fringes that contribute to the additional valleys shown in figure 6(a). Two signal processing algorithms, one based on time-gating the time-

domain signal and the other based on direct filtering of the S11 parameter, were developed to extract the antenna resonant frequencies from these signals.

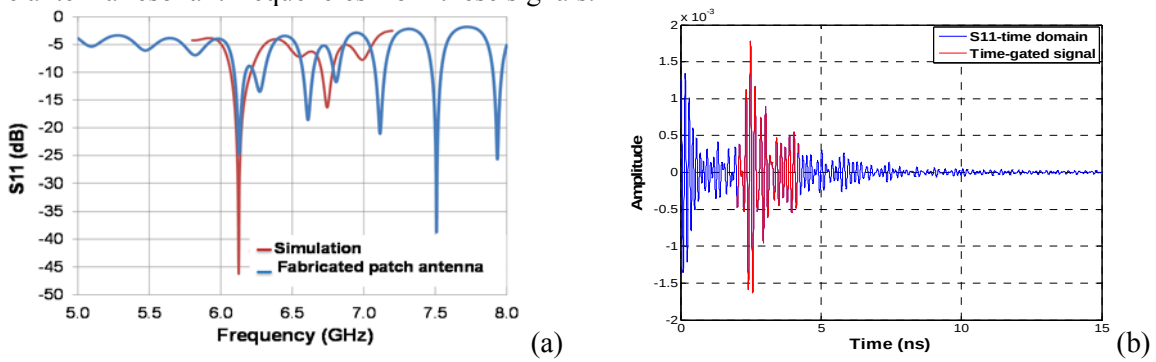

(a) (b)

Figure 6: Signals acquired from the antenna sensor with a long transmission line; (a) as-acquired S11 parameter displays multiple valleys; (b) time-domain signal calculated from the S11 parameter shows the reflections at the connector and by the antenna patch.

3) Develop fabrication techniques to embed antenna sensors in custom-made prosthetic liners: two different techniques were investigate to embed antenna sensors in custom-made prosthetic liner: (i) *casting the liner using a mold*: an eight-part mold was designed and fabricated using 3D printing technique. The design of the mold is shown in figure 7(a) and a picture of the 3D printed mold is shown in figure 7(b). The mold consists of an inner part and an outer shell; the inner part is a tapered cylinder while the outer shell has four separable part. When assembled, the inner part is centered inside the outer shell with a 6 mm gap between these two parts. Silicone was poured into the cavity between the cone and outer mold and allowed to cure fully. To remove the cured liner from the mold, the outer shell of the mold were separated so that the liner can be released from the inner part. As the 3D printed parts have a rough surface and tiny open pores, high grade sandpapers were used to polish the surfaces to achieve a super smooth surface. In addition, high temperature spray was used to seal the pores. Prior to pouring the silicone, the surfaces were also coated with a release agent, Ease Release® 200, for easier releasing of the liner from the fixture. A picture of the liner fabricated using this technique is shown in Figure 7(c). Two antenna sensors were embedded in the prosthetic liner. Because the antenna sensors were made on flexible substrates, a mechanical reinforcement was implemented to increase the rigidity of the sensor at the SMA connector. However, we found that it was difficult to put the liner on using the conventional rolling technique because of this reinforcement. In addition, the sensor can be easily broken when we tried to fold the liner.

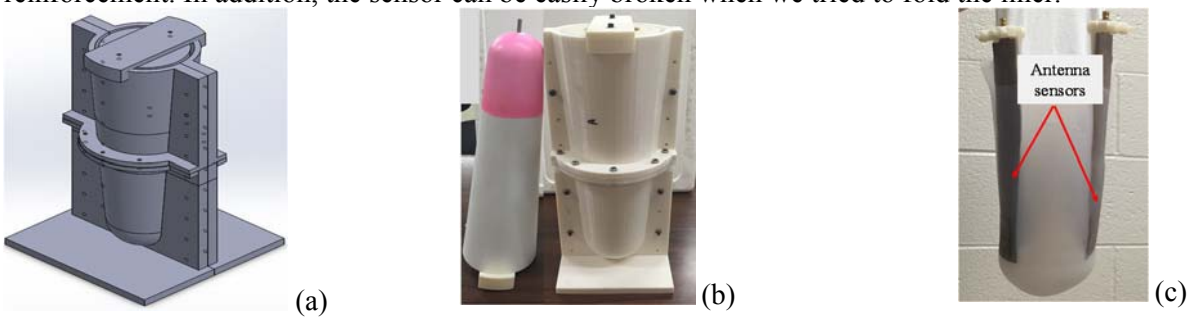

(a) (b) (c)

Figure 7: Embed antenna sensors in custom-made prosthetic liner (technique #1); (a) design of the mold for liner fabrication; (b) 3D printed inner and outer mold; (c) fabricated prosthetic liner with embedded antenna sensors.

(ii) *Casting the liner in sheet form*: a trapezoid mold was made to fabricate a sheet of silicone with the antenna sensors embedded, as shown in figure 8(a). Prior to the casting, the locations of the antenna sensors relative to the limb were measured so that the antenna sensors can be placed in the mold

properly. After the silicone sheet was released from the mold, it was draped over the limb of the volunteer with the antenna sensors aligned at the desired locations. The silicone sheet was then trimmed and connected together using Velcro strips to form the liner, as shown in Figure 8(b). A picture of the liner worn by a volunteer is shown in Figure 8(c) and a picture of the volunteer wearing the liner inside a socket is shown in Figure 8(d).

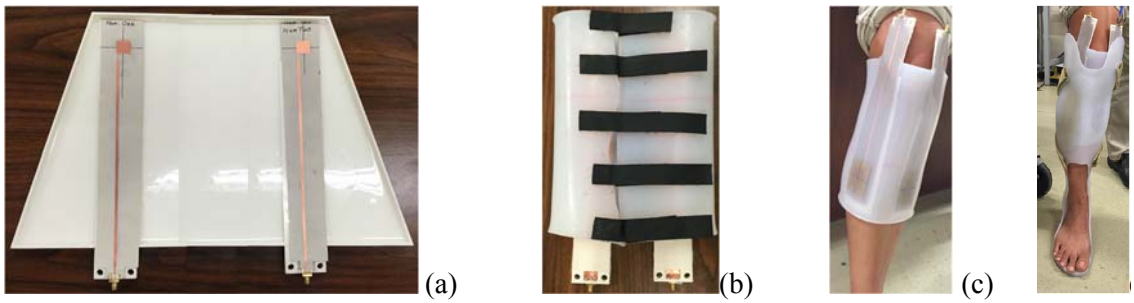

(a) (b) (c) (d)

Figure 8: Embed antenna sensors in custom-made prosthetic liner (technique #2); (a) fabricate the liner in a sheet form; (b) trimming and forming of the liner using Velcro straps; (c) the liner wore by a volunteer; (d) the liner inside a socket wore by a volunteer.

- **Significant results**: to determine the resonant frequencies of the antenna sensor with a long transmission line, two digital signal processing algorithms were developed. The first algorithm converts the measured S11 parameter to a time-domain signal first and then performs time gating to remove the signal reflected by the connector. The antenna resonant frequencies can then be determined from the spectrum of the time-gated signal, as shown in figure 9(a). In addition, due to the long transmission line, the interference fringes are periodical with a high frequency component. Therefore, filtering the S11 signals using a low-pass filter can remove these high frequency components, as shown in figure 9(b). Both methods can be implemented in hardware in the future.

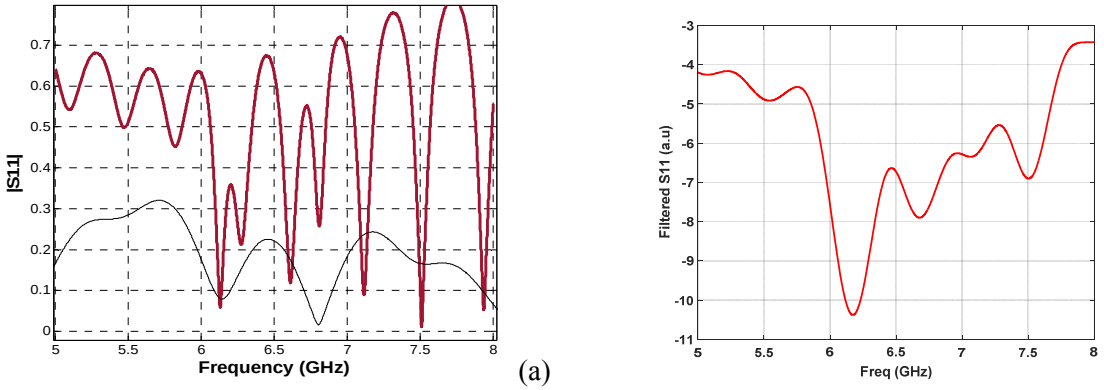

(a) (b)

Figure 9: Extracting antenna resonant frequencies from the measured S11 parameter; (a) spectrum of time-gated signal; (b) filtered S11 signal.

Using a Vector Network Analyzer, data were collected from the sensors embedded inside the liner at different fitness of the socket, e.g. very loose, loose, tight, and very tight. As shown in figure 10, small frequency changes were observed from the sensor data. A calibration procedure will be developed in the future to correlate the frequency shifts to the pressure and shear stresses experienced by the limb.

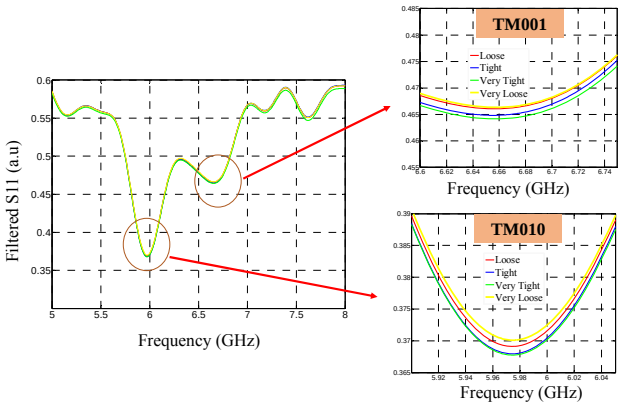

Figure 10: S11 signals collected from the sensor embedded in the custom-made liner at different fitness of the socket.

Accomplishment #3: Develop portable sensor interrogation system for dynamic data acquisition

- **Specific objective:** realize a compact interrogator that can measure the resonant frequencies of the antenna sensor at a fast rate of around 200 Hz
- **Major activities**:

1) Design and fabricate an FMCW signal generator: the VNA commonly used for measuring the S11 parameter of the antenna sensor is too bulky and too slow if we want to test the antenna sensor during walking. In order to achieve dynamic interrogation of the antenna sensor, an FMCW signal generator is implemented by using a Voltage Controlled Oscillator (VCO). Supplying a saw-tooth signal as the control voltage, the instantaneous frequency of the VCO output is swept through a frequency range continuously during each period of the saw-tooth signal. The sweeping rate and the frequency range of the chirp signal can be adjusted by changing the frequency and the amplitude of the saw-tooth control signal. The block diagram of an FMCW signal generator is shown in figure 11. A periodic saw-tooth signal is firstly generated using a 555 timer chip (TLC555). This signal is amplified before it is supplied to the VCO. A frequency triplexer increases the frequency of the VCO output to 5.1 to 6.9 GHz. In order to minimize the circuit size, all the electrical components of the FMCW signal generator are surface mounted and soldered on the PCB board. The fabricated circuit is shown in figure 11(b). The entire PCB FMCW transmitter has a total power consumption of the circuit is around 160 mW.

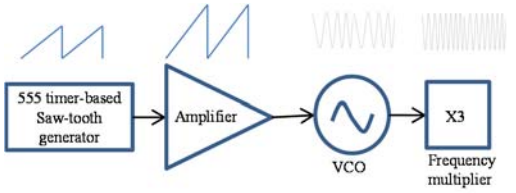

(a)

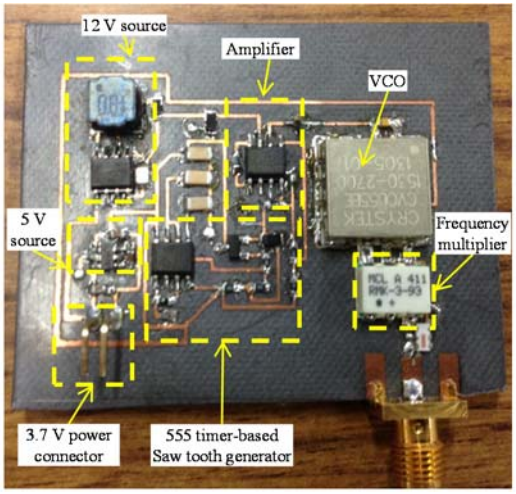

(b)

Figure 11: FMCW signal generator; (a) circuit diagram; (b) hardware implementation.

2) Realize an integrated portable interrogation unit: the block diagram of the interrogator is shown in figure 12(a). The FMCW signal is first filtered using a band pass filter to remove the harmonics and then is routed toward an antenna sensor using a circulator. The signal reflected by the antenna sensor is routed by the circulator to a power detector, which produces a direct-current (DC) signal that is proportional to the input power. Finally, this DC signal is measured using an ARM-based microprocessor, which also acquires the saw-tooth sync signal simultaneous. A shield for the microprocessor was implemented using a prototype board that is 6.3 inch long and 4 inch wide, as shown in Figure 12(b). The FMCW-based signal interrogation circuit was mounted on the prototype board with pins connected to the micro-processor board through pin headers. A rechargeable USB battery is used to power the micro-processor board, which in turn provides power to the FMCW-based interrogator. The shield also has a microSD card holder for data storage and a Bluetooth radio for communication to a smart device. A 3D printed plastic box was made to house the interrogator.

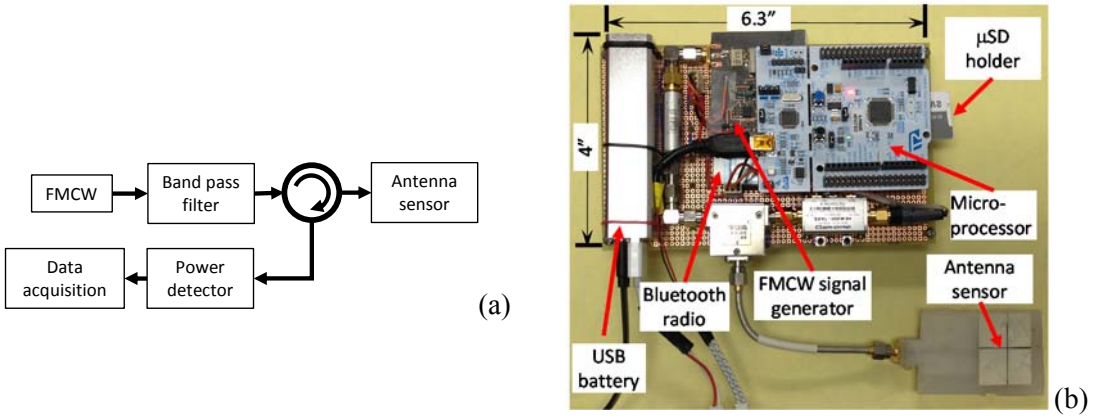

Figure 12: portable interrogator for antenna sensor; (a) block diagram; (b) hardware implementation.

3) Develop firmware for real-time data acquisition, processing, and storage: a microprocessor specific firmware was developed. The firmware enables three operation modes: 1) acquire the signals for a given period of time and transmit the signals to a Bluetooth device wirelessly; 2) acquire the signals and store the data on the microSD card continuously; 3) acquire the signal, process the signal to determine the antenna resonant frequencies, and transmit the antenna resonant frequencies wirelessly. For the first two modes, the microprocessor can acquire the signals at a sampling rate of 600 k sample/second. For the third mode, the sampling rate needs to be reduced in order to avoid missing data.
4) Develop an Android program for wireless communication with the sensor interrogator: an android program was developed to enable control of the sensor interrogator using a smart device. The program also enables the smart device to receive and display the data transmitted by the sensor interrogator.

- **Significant results:** the sync signal and the sensor signal acquired by the microprocessor is shown in figure 13(a). The two peaks of the power detector output for each saw-tooth cycle correspond to the antenna resonant frequencies. The antenna frequencies can be determined as the voltage of the sync signal at the location of the two peaks, as shown in figure 13(b). The variations of the voltage correspond to a frequency variation of 25 MHz. The cause of this large variation needs to be investigated in the future.

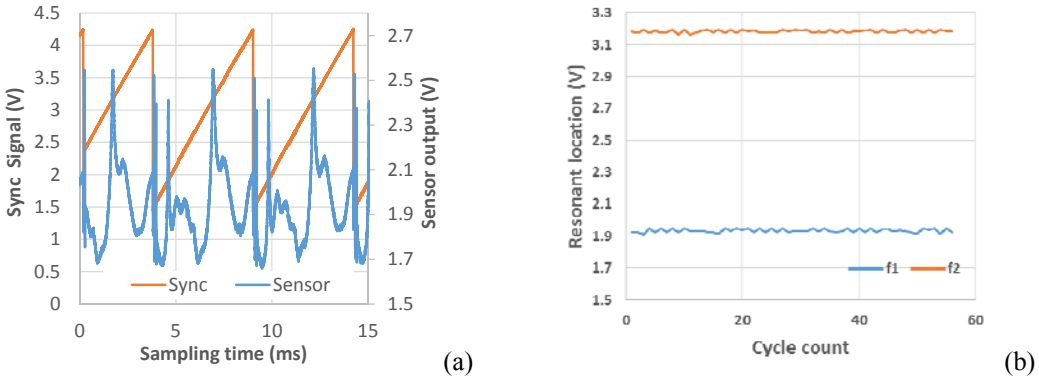

(a) (b)

Figure 13: (a) The sensor signal and the FMCW control voltage collected by the fast data acquisition unit. (b) the peak locations detected from the collected data.

Accomplishment #4: Fabricated an anatomically accurate dynamic limb-socket interface to record and modulate the load tolerant areas during simulated walking conditions

- **Specific objectives:** 1) build a prosthetic socket with recessed pockets and externally routed airlines for the integrated actuator inserts to provide a flush surface clear of obstruction for the load bearing areas; 2) investigate and modulate loading at the limb-socket interface during simulated walking experiments
- **Major activities**:

1) A thermoplastic socket was formed by the UT Southwestern Prosthetics and Orthotics Lab to accommodate the actuator inserts at load tolerant areas. Airlines were then routed through external ports to achieve a flush profile within the socket (see figure 14 (A) and (B)).
2) The limb insert was sensorized using two F-socket force sensors at the anterior, lateral, and medial load bearing areas.
3) Two sets of experiments were performed to understand the interface behavior during simulated walking.
    a. First, the sensorized limb was loaded with 23 kg of weight and inserted into the uniformly inflated prosthetic socket where the gait cycle was simulated by rolling the limb-socket interface between the toe-off and heel-strike positions at defined intervals of 5 seconds. Changes in the interface pressure and the internal air pressure of the actuators were captured throughout these simulations. Our loading process proceeded as follows: the limb is inserted into the socket while the inserts are at atmospheric pressure and left uninflated, the inserts are then inflated to a uniform set pressure of 41 kPa, a weight of 23 kg is then place on top of the residual limb to simulate body weight.
    b. Secondly, the experiment included modulation of the internal air pressure in the anterior actuator insert. While held in the toe-off position, the individual air cells within an insert were returned to a uniform pressure after experiencing unequal changes. This was performed to examine the effect on load distribution at these extremities within the gait. Our loading process for this experiment proceeded as follows: the limb is inserted into the socket while the inserts are at atmospheric pressure and left uninflated, the inserts are then inflated to a uniform set pressure of 41 kPa, a weight of 23 kg is then place on top of the residual limb to simulate body weight, and finally the air cells are readjusted back to 41 kPa before roll-over testing begins.
4) A testing apparatus was constructed to control the tilt degree and path of the limb-socket interface while simulating walking (see figure 14(C))

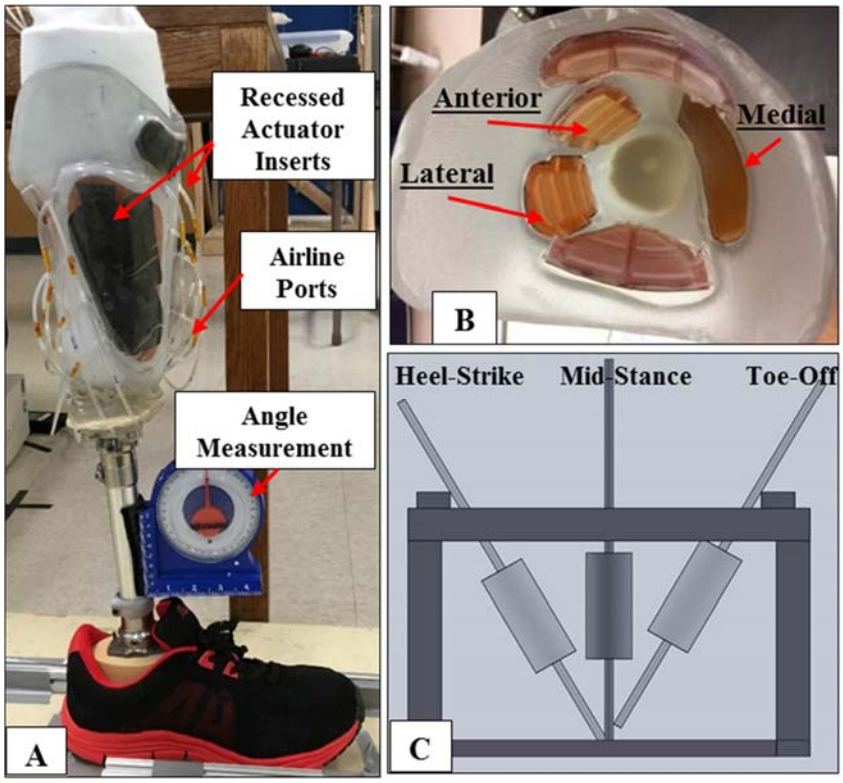

Figure 14: (A) The limb-socket interface with recessed pockets for actuator inserts and airline ports to connect the individual air cells with the control unit. An attached angle measurement device has been used in the test to derive the degree of tilt when performing the roll-over test. (B) The inside of the modified prosthetic socket shows uninflated actuator inserts flush with the sidewalls of the socket. Our test results have primarily focused on the lateral, anterior, and medial load bearing areas. (C) Further roll-over testing will be conducted using a recently constructed test platform which guides both the degree of tilt and path of the limb-socket interface while translating between the toe-off and heel-strike positons.

- **Significant results:** the modified socket incorporates actuator inserts at load bearing areas which can be inflated and deflated to modify and reduce the peak interface forces experienced by the fabricated residual limb. In the laboratory setting, this is verified by monitoring both the internal air pressure of the actuator inserts as well as the load sensors placed across the residual limb. Figure 15, representing data from the first test, shows that as the limb-socket interface was exercised through a simulated gait, the internal air pressure and interface forces experienced by the inserts was observed cyclically varying, reaching highs and lows at the toe-off and heel strike positions. Figure 16, representing data from the second test, indicates that when the interface pressure is set to a uniform pressure after bearing weight, the force distribution across the air cells is more evenly distributed. Extremities in the loading profile could be alleviated even further by adjusting high and low air pressure beyond uniform pressure to help improve fit and distribute the load more evenly across the load bearing areas.

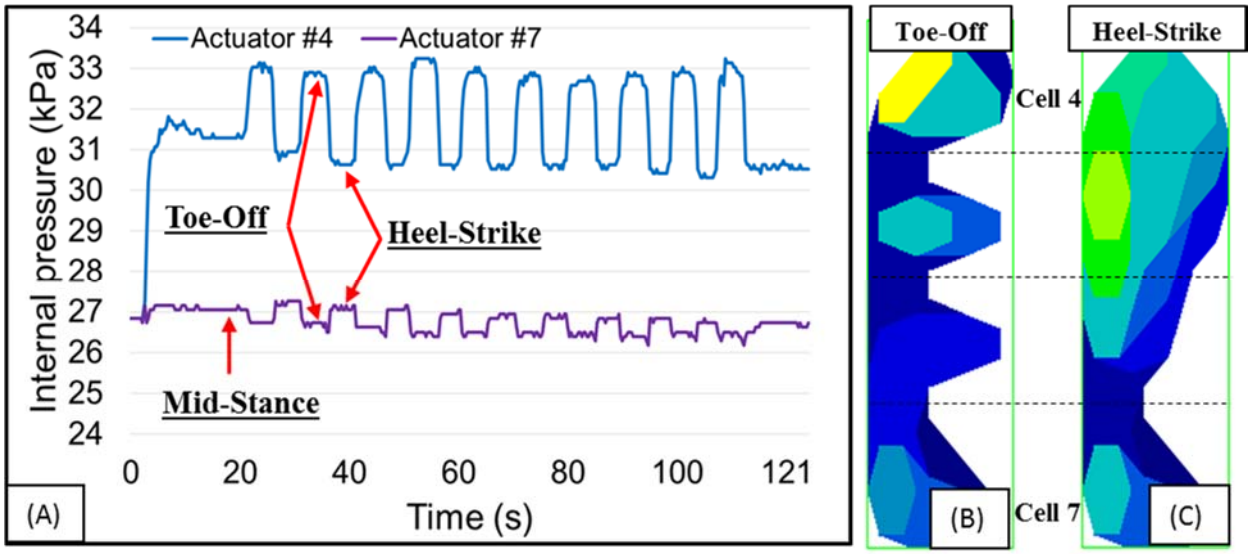

Figure 15: (A) The internal pressure of two actuator insert cells from the first set of testing is displayed showing the rise and fall of internal pressure as the weighted limb-socket interface is shifted between the Toe-Off and Heel-Strike positions; (B) As can be seen in the interface force display of the actuator insert in the Toe-Off position, the load is concentrated onto the top cell of the insert; (C) As the limb-socket interface shifts to the Heel-Strike position, the load concentrated at the top of the insert shifts to down revealing that the fit of this prosthetic socket could be improved to accommodate for this change in interface pressure. Furthermore, internal pressure relief of the top cell in the Toe-Off position could be performed to better distribute the load across more of the actuator insert cells.

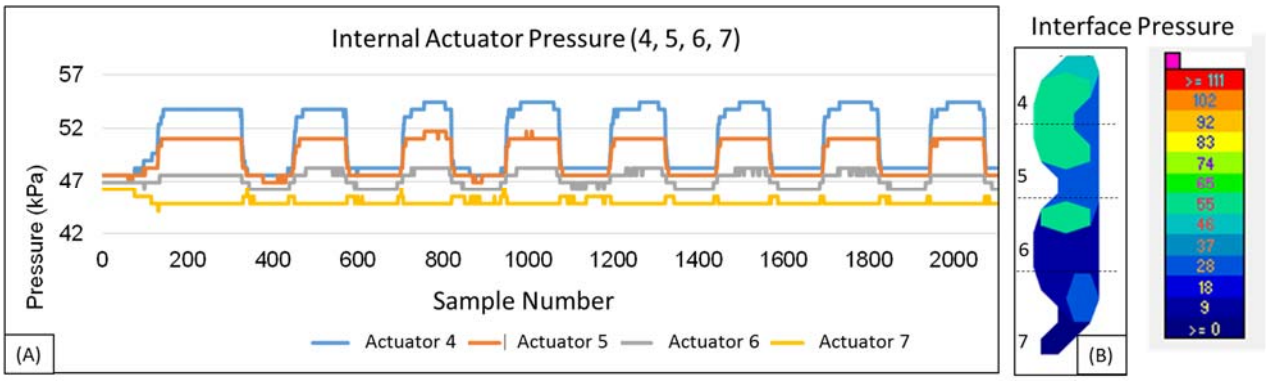

Figure 16: (A) the internal air pressure of four actuator insert cells from the second test is shown rising and falling with the translation between the heel-strike and toe-off positions. It should be noted that their initial pressure is very close as the air pressure was uniformly redistributed after the load of 23 kg was placed. (B) The resulting interface pressure at the toe-off position shows that despite similar conditions, returning the air pressure of the actuator inserts to uniformity after load bearing improves the even distribution of weight across these areas.

Accomplishment #5: Integrated inflatable actuator insert technology into a custom made Patellar Tendon-Bearing Ankle Foot Orthotic (PTB-AFO) and performed walking analysis with a healthy volunteer

• **Specific objectives:** 1) Fit a healthy volunteer with a PTB-AFO modified to include the actuator inserts in recessed pockets; 2) test the loading conditions and comfort level of the system while walking; 3) assess the capability of the system to modulate interface pressure while walking.

• **Major activities**:

1) A custom fitted PTB-AFO device was made to transfer most of the body weight of a healthy volunteer onto the patellar tendon and along the medial/anterior load bearing areas so that a below-knee amputation could be imitated. Fabrication of PTB-AFOs for two healthy volunteers was performed by the UT Southwestern Prosthetics and Orthotics Lab and accommodations were made to integrate inflatable actuators into load bearing areas.
2) To examine load distribution, F-Socket sensors were attached at load bearing areas to a sleeve fitted around the leg of a healthy volunteer as seen in Figure 17(A). The PTB-AFO device with embedded actuator inserts was then fastened to the sensorized leg of the volunteer. In two separate tests, the system was inflated to an initial pressure of 27 kPa and 42 kPa while offloading the volunteer's weight by standing on the opposite leg. This ensured that the required displacement of the actuator inserts was reached. As seen in Figure 17(B), walk testing was conducted on a treadmill set at a constant pace of 0.89 m/s for a duration of 180 s. During this time, the interface pressure and internal air pressure of the anterior, lateral, and medial load bearing areas were recorded.
3) Further testing was conducted in a second series of tests attempting to modulate the interface pressure of the system while walking. In this trial, all actuators were inflated to an initial pressure of 41.4 kPa and the volunteer walked on the treadmill for approximately 180 s at a pace of 0.89 m/s. Periodically, the volunteer was asked to pause in the toe-off position while the highest internal pressures of the actuators were relieved down to that of their neighboring cells and the resulting pressure profile of the socket was recorded.

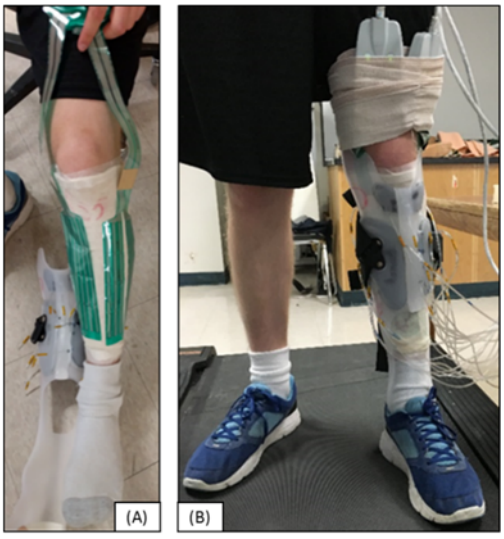

Figure 17. The PTB-AFO Test: (A) The leg of the healthy volunteer is shown covered in a sock with attached F-Socket load sensors; (B) The first iteration of the PTB-AFO on a treadmill with air and F-Socket communication lines leading to a tabletop test setup close by.

• **Significant results:** Two sets of treadmill experiments were performed with the PTB-AFO: a) The PTB-AFO device with integrated actuator inserts enables us to monitor and modify the pressure profile across the surface of a user's leg which can improve fit and force distribution throughout the gait cycle. Our first set of experiments concluded that the force and internal pressure of the device was recorded successfully and that the device could be worn comfortably. While the interface pressure distribution across some areas showed high variance, others showed very little variation

throughout the gait cycle possibly indicating that the fit of the PTB-AFO or its inserted actuators needs to be adjusted further for a greater effect on pressure distribution across such areas; b) modulation of the pressure profile while walking proved to be relatively ineffective as the portable system used in the second set of experiments lacked the capability to record and adjust the pressure profile of individual cells within the space of a single step. When attempted, the overall change in the pressure profile was seen to be minimal and it was suggested that re-adjustment should be done while pausing walking and can be performed only occasionally as needed. While the initial goal of modulating the interface pressure during the gait cycle proved to be unachievable with this current setup, we envisioned a protocol capable of improving the fit of a prosthesis by occasionally pausing the gait to allow the system to re-adjust pressures to their desired values.

Accomplishment #6: Consolidated the actuator insert control system into a portable device while reducing its weight and adding new features and functionality.

- **Specific objectives:** 1) develop a portable control unit capable of mapping, modulating, and automatically regulating actuator array pressure; 2) test the efficacy and usability of the portable system on a healthy volunteer while walking on a treadmill
- **Major activities**:

1) Addressed electrical reliability issues with the solenoid driver circuit mentioned in the 2015 annual report.
2) Reconfigured the tabletop pneumatic control unit into a wearable system capable of being carried in a backpack. The tabletop based pneumatic control system was useful for preliminary hardware testing; however, a few aspects of this device required changes in order to realize a portable version of the system for further testing. First, in order to convert the control unit into a wearable device, the electrical and electronic components of the control unit were rearranged to fit into a backpack, as shown in figure 18. Next, the air channels were aligned with their corresponding pressure transducers and routed to their respective actuator cells. Additionally, the functionality of the system was consolidated into a single microcontroller unit and a switch circuit for the pump, power circuit, new pressure regulator, and Bluetooth module were added.
    a. Consolidated the input and output functions into a single microcontroller board. The features and capabilities of the previous system included separate devices for the input and output functions. Earlier, data acquisition from the pressure sensors was carried out by a NI cRIO-9074 chassis via a NI 9205 module while actuation was controlled by an Arduino microcontroller board. In order to reduce the size and weight of the system, both of these functions were integrated into a single Arduino microcontroller board. This enables the microcontroller the ability to directly modulate its actuator pressure based on its own reading of the pressure profile as opposed to previous efforts where commands were received by a connected computer. This has led to a more autonomous system which is easier to deploy, less complex, and more reliable in its testing. Functionally, the updated controller design requires less time for its initial setup and starts the inflation process sooner in comparison to previous efforts.
    b. Improved control over the pump by adding a programmable switch to turn the air pump on/off as required by the system based on the pressure profiles. This allows for reduced power consumption, reduced load on the motor, and reduction in the duration of noise generated by the pump.
    c. An on-board switch mode power supply was integrated into the system to draw +9V from the main +24V power supply input to power the miniature diaphragm pump. Additionally, a voltage regulator was added to provide a +5V supply to the sensors.
    d. The OEM-EP miniature pressure regulator has been replaced by a QPV1 from Proportion Air in order to overcome irregularities and inconsistencies observed in the former regulator. This regulator has also provided a faster response to command signals by attaining a steady state pressure quicker than the previous regulator.

e. Bluetooth has been added into the system to wirelessly communicate with the GUI and reduce future tethering and data lines.
f. Determined a multipoint calibration curve for the pressure regulator in order to achieve better accuracy upon reaching the set point pressure.

3) Conducted PTB-AFO testing with the portable control system packed into a backpack tethered by power, data, and air lines at the time of testing. Subsequent configurations of this system have reduced these requirements down to needing only a power line for future testing.

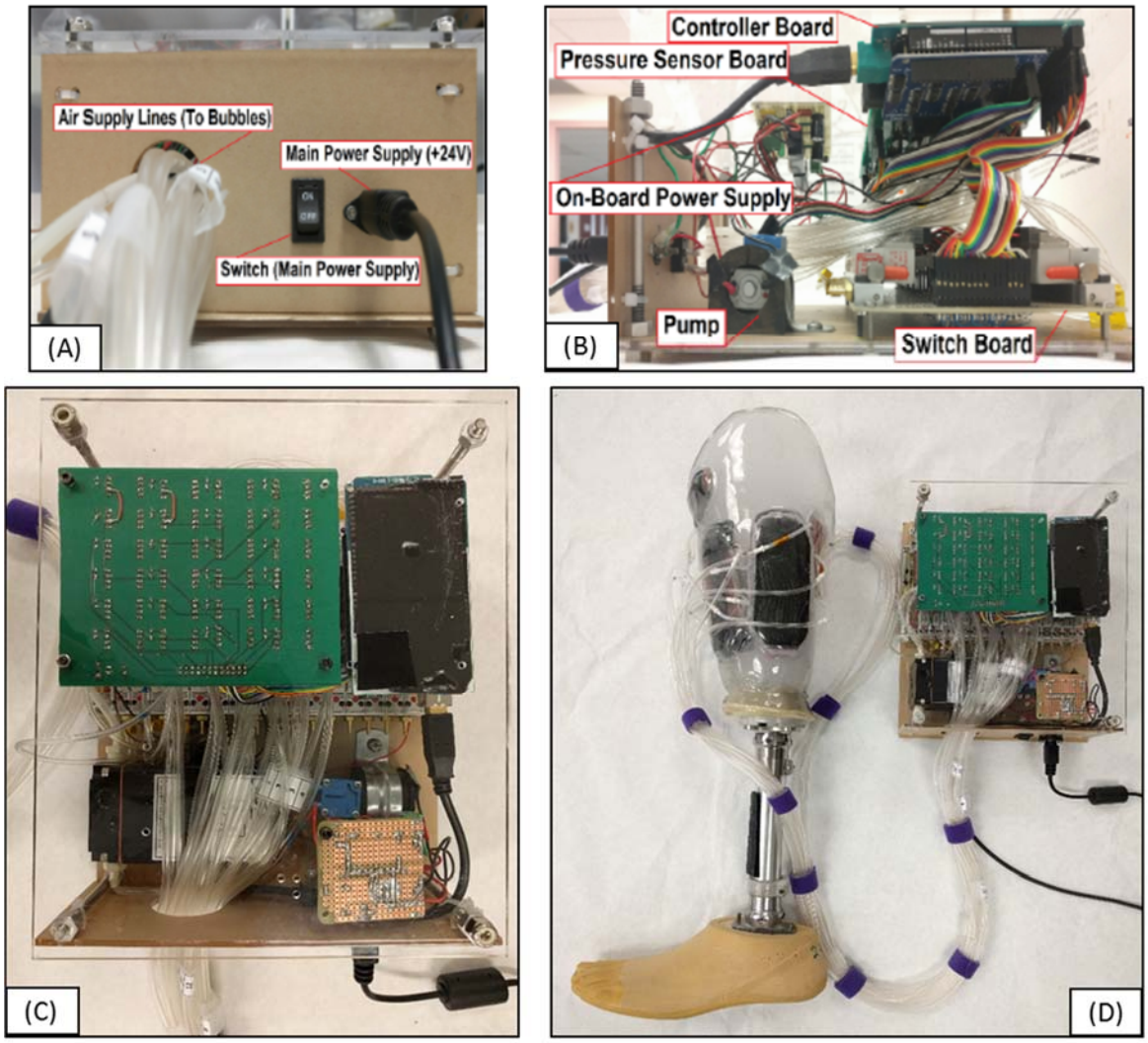

Figure 18: Control system for the Prosthetic Interface; (A) Front panel view with bundled air lines, main power switch, and power supply line; (B) Inside view showing the arrangement of the pump, switch board, microcontroller board, pressure sensor board, and power supply; (C) Outside view showing the acrylic frame housing the assorted electronics (D) Integration with the prosthetic socket showing bundled air lines routed to their respective actuator cells.

- **Significant Results:**

1) By reducing the number and size of components, the weight and size of the whole system were greatly decreased. With this improvement, the various components were then integrated into a small, portable package which provided a more robust test setup than the discreet components used before. This led to a system which is easier to deploy and more reliable in its testing. Additionally, it has

better potential to be used in various environments and in testing on treadmill, stairs, or open lab space.

2) The portable control unit has been tested using the PTB-AFO setup on a treadmill and has proven capable of actuating each air cell to a set internal pressure. As seen in Figure 19, at the time of testing the pressure regulator and air supply was kept outside the control unit. While maintaining and modulating the internal pressure was achievable with periodic offloading for re-adjustment, modulation of the air cells proved time consuming from an actuation standpoint as the pressure regulator took a significant amount of time settling at the set pressure value. As such, the pressure regulator was switched out with the faster settling QPV1 model and this issue was resolved. Additionally, both the pump and regulator have been moved on-board within the control unit.
3) Although the portable system can be carried in a backpack, it is still tethered by power and communication lines. This has led to an effort to convert the transmission of the air pressure data to a wireless method, specifically Bluetooth. This feature has been added and is awaiting testing. Additionally, an investigation into powering the system by battery has begun and is currently in its initial stages.

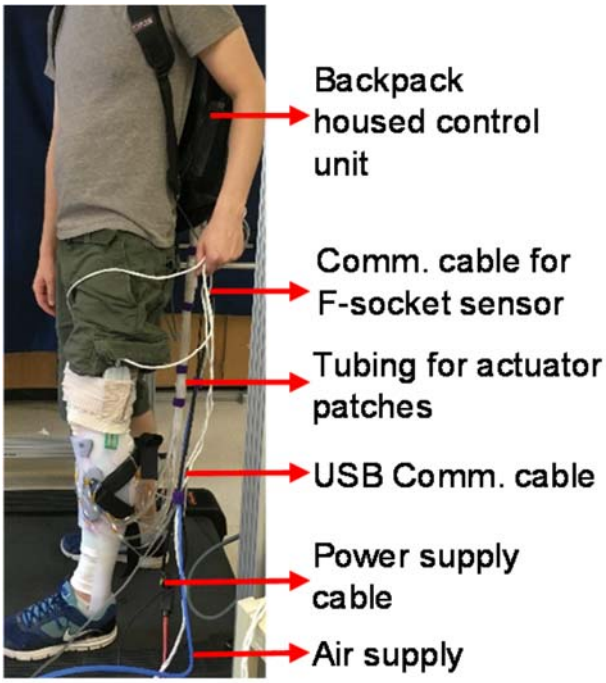

Figure 19: The treadmill PTB-AFO test where the control unit is carried within a backpack. Tubing between the control unit and PTB-AFO comes out from a hole in the bottom of the backpack. Externally connected lines in this test included the USB and F-Socket sensor cables for communication of the internal and interface pressures, power supply line, and an air supply leading to a regulator. The USB and air supply lines have since been removed and replaced with wireless and internal options, respectively. Plans to switch the power supply over to battery are currently in progress.

Accomplishment #4: Successfully ported the actuator insert control GUI to a C# environment so as to achieve greater data acquisition and actuation rates as well as provide a better user experience.

- **Specific objectives:** 1) provide a GUI capable of acquiring data and modulating the actuator insert control system fast enough to alleviate limb-socket interface loading throughout the gait cycle; 2)

Provide a responsive and intuitive user experience for testing which enables the user to adjust the interface pressure of the limb-socket while recording the resulting internal air pressure profile.

- **Major activities:**

1) Initial Matlab and LabView based GUIs were developed focusing on real-time visualization of the system's pressure profile, capturing internal air pressure data, and controlling individual air cells. Additional functionality was added to allow for user defined set-pressure maps so as to actuate the air cells in groups.
2) A new GUI was developed in C# which replicated the functionality and progress of the previous GUIs while providing faster data acquisition and actuation speeds. Its initial development, seen in Figure 20, shows how an internal air pressure profile is visualized using representations of the actuator air cells. With it, a user can individually modulate actuator pressures or load a pressure profile map.
    a. In order to achieve a better data acquisition rate with a single controller board, the capabilities of this GUI were developed on a Windows based platform using the C# language.
    b. The GUI provides a functional layout of the relevant controls and user inputs which include: configuration, communications, mode of operation, and units. It also depicts the location, number, and internal pressure of each cell of the inserts to match the prosthetic interface actuator layout as seen in the prototype prosthetic limb. This display reflects internal air pressure values with a change in color at the corresponding interface location as well as with an individual pressure value. Furthermore, the GUI provides functional groups, as shown in Figure 18, with the following controls: for data processing, the user may record pressure datasets along with timestamps to an excel spreadsheet; for actuator control, the user may set all actuator cells to a set pressure, edit pressure values of individual cells or of groups of actuator cells; for communication, the user may use a tethered serial connection such as USB or wireless Bluetooth communication; the display mode of the recorded values may be changed between units of kPa or PSI; Operation modes can be changed between a Default Mode to set the actuators to a single set pressure map and cease operation or Continuous Re-adjustment Mode which attempts to continuously maintain the pressure of the actuator cells at their defined pressure values.
    c. The system was programmed with a selectable Bluetooth option to allow transfer of actuator pressure data via wireless communication to the GUI. This was chosen to provide a more portable system during testing and potentially for future use by patients. The default mode of communication between the GUI and the control system is still set to Serial communication during our transition to a fully portable control unit.
    d. The system can now be set to continuously readjust the pressures of the actuators to a predefined pressure profile chosen by the user. This is a selectable user option in the Mode of Operation controls. The default mode of operation is set to inflate the actuators to the pressure profile set by the user and cease operation.

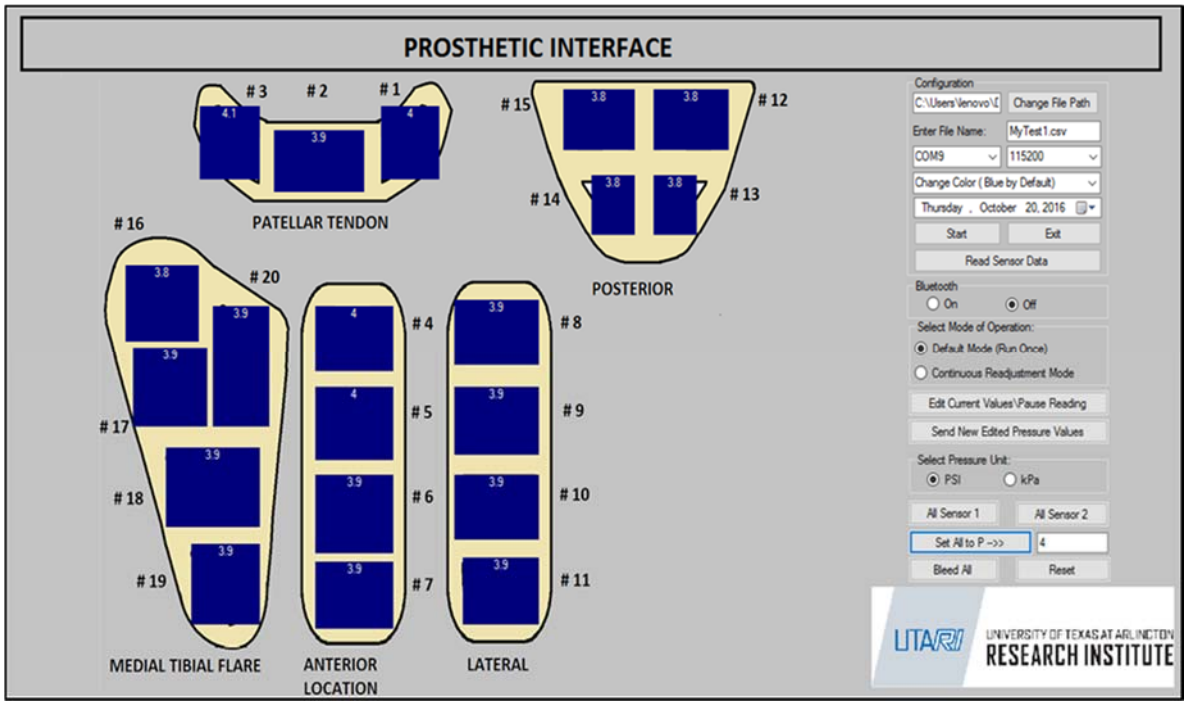

Figure 20. Current C# based GUI developed for data visualization, modulation, and recording of internal actuator pressures.

- **Significant results:**

1) Early testing performed with the initial Matlab and LabVIEW GUIs provided reasonable recording from the portable limb-socket interface controller but lacked the necessary data acquisition rate in order to decipher between individual positions of the gait cycle. Additionally, the actuation rate of the system was lacking when attempting to modulate the interface pressure while walking.
2) Within benchtop testing, we've confirmed the operations of the new C# based GUI when integrated with the control system hardware and prosthetic socket interface. It performs faster than the predecessor GUIs in both acquisition of data and actuation of the air cells. Further testing at UT SouthWestern is scheduled with human volunteers where the data acquisition and actuator modulation will be demonstrated.

- **What opportunities for training and professional development has the project provided?**

The project supported three graduate students and three research scientists. It offers a unique opportunity for the graduate students, the research scientists and the PIs to interact with medical researchers at UT Southwestern medical school and gain insights and knowledge related to prosthetics and orthopedics. A Master student graduated with the support of this grant. An undergraduate minority student is recruited to help with the mechanical design of the test fixture.

- **How were the results disseminated to communities of interest?**

The PIs presented research results at two conferences, i.e. the 9th ACM International Conference on Pervasive Technologies Related to Assistive Environments (PETRA 2016) and the 6th IEEE Conf. BIOROB. In addition, a Master thesis on the fabrication technique to embed the sensor in the prosthetic liner has been submitted to the UTA library. The PI also discussed the project with representatives from two start-up companies (MedHab in Fort Worth and a Chinese company) on potential license opportunities.

1. Huang, H., Yao, J. and , Eilbeigi, S., "Simultaneous Shear/Pressure Antenna Sensor", conference proceedings, The 9th ACM International Conference on Pervasive Technologies Related to Assistive Environments (PETRA 2016), Corfu Island, June 2016
2. Eilbeigi, S., "Embedding antenna shear/pressure sensors in prosthetic liner material", MS thesis, University of Texas Arlington
3. Carrigan W, Nothnagle C, Savant P, Gao F, Wijesundara MBJ, "Pneumatic Actuator Inserts for Interface Pressure Mapping and Fit Improvement in Lower Extremity Prosthetics," Proc. the 6th IEEE Conf. BIOROB, June 2016, Singapore

- **What do you plan to do during the next reporting period to accomplish the goals?**

1) Implement a test fixture for testing the prosthetic liner under conditions imitating the prosthetic socket;
2) Develop circumference and bio-impedance antenna sensors;
3) Embed antenna sensor array in prosthetic liners;
4) Modify the PTB-AFO airlines by running them in tracks along the outer surface of the device. This grouping will help better organizing the airlines and alleviating tension as well as swaying of the lines when walking.
5) Conduct further experimentation with the PTB-AFO and limb-socket test interface using the improved control system. The improved system, with both faster data acquisition and pressure modulation rates, will allow us to examine more closely the effect of pressure modulation within the steps of the gait cycles.
6) Test real amputee with gait pattern analysis to check for improvements
7) Investigate interface modulation methods to improve interface pressure reduction. This will include evaluating how improved fit can alleviate peak pressure and aid in reducing interface pressure variance during walking.
8) Improve the portable control system to include battery powered operation
9) Integrate shear and pressure sensors to allow for closed-loop feedback control

4 IMPACT

- **What was the impact on the development of the principal discipline(s) of the project?**

Validating the performance of the shear/pressure sensor provides a much-needed sensor technology to advance the smart control of prosthetic socket. The development of the portable sensor interrogator will enable measuring the interface stresses during walking. These capabilities will offer a physics based objective instrument to evaluate the current practices of prosthetic fitting. The realization of flexible sensors implemented in prosthetic liners will lead to low-cost smart liners that are comfortable to wear on a daily basis. The studies of the air cell actuator will enable more precise adjustments of the prosthetic fitting at targeted areas.

- **What was the impact on other disciplines**

The sensor and actuator technologies developed in this project as well as the methods used to alleviate interface pressure can be easily adapted for other applications, such as diabetic foot monitoring, wheelchair cushions, hospital beds, pillows, etc. The development of the compact low-cost sensor interrogator remove a major technology barrier that hinders the extension of the flexible antenna sensor for other applications, such as Structural Health Monitoring and wearable devices.

- **What was the impact on technology transfer?**

A US patent titled "Sensor assembly, method, and device for monitoring shear force and pressure on a structure" has been granted (#9138170 B2). UTA Technology Management Office has been actively seeking license opportunities for this technology.

- **What was the impact on society beyond science and technology?**

None to report.

5 CHANGES/PROBLEMS

- **Changes in approach and reasons for change**

The design of the antenna sensor is changed so that one antenna sensor can simultaneously measure shear and pressure, which makes the antenna sensor much simpler. After discussing with the researchers at UT Southwestern Medical School, we decided to explore the implementation of the antenna sensors on the prosthetic liner, which is more practical and require less modification of the prosthetic socket.

- **Actual or anticipated problems or delays and actions or plans to resolve them**

The recruited students were again denied visa and two master students decided to quit the project because of degree plan change at UTA. A research associate and a master student are recruited. One PhD student is recruited and currently supported with the department teaching assistantship.

The silicone material with properties similar to commercial liners can only be purchased in large volume. Substantial amount of time was spent on testing different silicone materials. A substitute silicone material from Smooth-on is found and the sensor need to be recalibrated. In addition, we are evaluating foam material as the spacer between the patch antenna and the reflector to improve the sensitivity of the sensor.

It was discovered during our PTB-AFO testing that the data acquisition rate we achieved using the setup at the time would be insufficient to analyze the individual steps of the gait cycle. This was due to two factors: first, the GUI's communication protocol was not optimized for continuous data output and second, the automated system meant to maintain the air pressure in the cells was having to wait for the air pressure regulator to reach a settled value which was very time consuming with the regulator in use. Our solutions to data acquisition have been to switch our platform over to a C# based GUI with easier optimization options to configure the communication protocol. Actuation has been improved by swapping the slow air pressure regulator out with the faster QPV1 model. The efficacy of these changes will be demonstrated in the next quarterly report.

- **Changes that had a significant impact on expenditures**

Delay in hiring graduate students due to visa issues.

- **Significant changes in use or care of human subjects, vertebrate animals, biohazards, and/or select agents**

None.

6 PRODUCTS

- Two conference papers;
- One Master thesis;
- Project description at the PI's website (astl.uta.edu);
- One patent granted (US9138170 B2);
- A portable sensor interrogation unit with 200 Hz sampling rate;
- A test fixtures for characterizing antenna sensor fabricated using soft liner material;
- Techniques for fabricate sensors on customized prosthetic liners;
- An anatomically correct limb-socket test setup for simulating amputee walking;
- Actuator inserts made to match the size and shape of load tolerant areas;
- A portable pneumatic control system for measuring and adjusting internal pressures;

- A user interface allowing for the implementation of automated inflation schemes and display of read pressures across the actuator inserts.

7 PARTICIPANTS & OTHER COLLABORATING ORGANIZATIONS

- **What individuals have worked on the project?**

Name: Haiying Huang
Project Role: PI
Researcher Identifier (e.g. ORCID ID):
Nearest person month worked: 3
Contribution to Project: Advise students and develop the dynamic sensor interrogation unit

Name: Shahnavaz Eilbeigi
Project Role: Graduate Research Assistance
Researcher Identifier (e.g. ORCID ID):
Nearest person month worked: 11
Contribution to Project: Investigate sensor fabrication technique

Name: Mohammadhesam Hajighasemi
Project Role: Graduate Research Assistance
Researcher Identifier (e.g. ORCID ID):
Nearest person month worked: 6
Contribution to Project: Develop control unit for the shear/pressure tester

Name: Hamed Tavakoli
Project Role: Graduate Research Assistance
Researcher Identifier (e.g. ORCID ID):
Nearest person month worked: 3
Contribution to Project: develop Android user interface for the sensor interrogation unit

Name: Hamed Tavakoli
Project Role: Graduate Research Assistance
Researcher Identifier (e.g. ORCID ID):
Nearest person month worked: 3
Contribution to Project: develop Android user interface for the sensor interrogation unit

Name: Farnaz Farahanipad
Project Role: Graduate Research Assistance
Researcher Identifier (e.g. ORCID ID):
Nearest person month worked: 2
Contribution to Project: Characterize sensor performance

Name: Elmira Ghahramani
Project Role: Volunteer (support with department teaching assistantship)
Researcher Identifier (e.g. ORCID ID):
Nearest person month worked: 1
Contribution to Project: fabricate sensors

Name: Muthu Wijesundara
Project Role: Co-PI
Researcher Identifier (e.g. ORCID ID):
Nearest person month worked: 2 (For the second year of the project)

Provide the guidance on test design and configuration

Name: Wei Carrigan
Project Role: Researcher
Researcher Identifier (e.g. ORCID ID):
Nearest person month worked: 3 (For the second year of the project)
Contribution to Project: Built test setup and performed test and data analysis

Name: Caleb Nothnagle
Project Role: Researcher
Researcher Identifier (e.g. ORCID ID):
Nearest person month worked: 3 (For the second year of the project)
Conduct PTB-AFO testing, developed the control system programming and setup

Name: Manish Guar
Project Role: Student Intern
Researcher Identifier (e.g. ORCID ID):
Nearest person month worked: 1 (For the first year of the project)
Contribution to Project: Develop control system setup

- **Has there been a change in the active other support of the PD/PI(s) or senior/key personnel since the last reporting period?**
  Nothing to Report

- **What other organizations were involved as partners?**
  Organization Name: The Ohio Willow Wood Company
  Location of Organization: Mt. Sterling, Ohio
  Partner's contribution to the project: technical consultant

8 SPECIAL REPORTING REQUIREMENTS

Quad chart (see appendix)

9 APPENDICES

- Quad chart
- Two conference paper

Simultaneous Shear/Pressure Antenna Sensor

Haiying Huang
University of Texas Arlington
500 W. First Street
WH211

Jun Yao
University of Texas Arlington
500 W. First Street
WH211

Shahanavaz Eilbeigi
500 W. First Street
WH211

ABSTRACT
This paper presents the development of a simultaneous shear and pressure sensor as well as its battery-powered interrogation unit. Based on the principle of multi-layer microstrip antenna, the shear/pressure sensor consists of a microstrip patch antenna and a U-shaped director, separated from the radiation element of the patch antenna using a layer of prosthetic liner material. We demonstrated that the shear and pressure displacements of the U-shaped director can be simultaneously measured from the two fundamental frequencies of the microstrip antenna. To make the shear/pressure antenna sensor feasible for prosthetic socket monitoring, a battery powered portable interrogation unit was developed, which can detect the antenna resonant frequencies at a high sampling rate of 190 Hz.

CCS Concepts
• Hardware→Sensor devices and platforms • Computer systems organization→Embedded and cyber-physical systems→Sensors and actuators.

Keywords
Shear/pressure sensor; prosthetic devices; antenna sensor; patch antenna; FMCW interrogator

1. INTRODUCTION
Prosthetic users frequently experience discomfort and skin problems, including irritation, blistering, skin breakdown, and ulceration, etc. (Meulenbelt et al. 2011; Meulenbelt et al. 2006). It is extremely difficult to address these problems due to two reasons; first, the exact causes of skin problems are not clearly understood (Sanders 2000). For example, it is well known that both pressure and shear stresses contribute to skin problems but the "safe" stress level, i.e. the stress level that will not cause skin problems, is not defined (Sanders 2000; Mak et al. 2001; Mak et al. 2010). In addition, the volume of the residual limb changes throughout the day. The unavoidable fluctuation of the residual limb volume in turn changes the fitting of the prosthetic device. In other words, even if the prosthetic device fits perfectly at the clinical visit, the fitting of the prosthetic device could change during the day and over time due to the residual limb volume changes. Prosthetics users frequently add or remove socks to adjust the fit of the prosthetics. This manual adjustment is not precise and cannot completely restore the initial setting of the prosthetics (Sanders et al. 2002). In order to adjust the prosthetic socket dynamically, we need an in-socket sensing system that can measure the interface stresses at real-time.

Currently, only interface pressure can be conveniently measured during ambulation. Despite of active researches in the past (Appoldt et al. 1970; Sanders et al. 1992; Sundara-Rajan et al. 2012), there is a lack of real-time shear sensors for prosthetic devices. In this paper, we will present the implementation and characterization of a simultaneous shear/pressure sensor as well as a fast sensor interrogation circuit that is suitable for dynamic monitoring of interface stresses.

2. PRINCIPLE OF OPERATION
A microstrip patch antenna is an electromagnetic (EM) resonator that can radiate or receive EM signals at specific frequencies. It usually consists of three components, namely a radiation element, a dielectric substrate, and a ground plane, as shown in Figure 1(a). The antenna resonance frequencies can be identified by plotting the return losses of the patch antenna as a function of the incident frequency, i.e. the S11 curve. As shown in Figure 1(b), a microstrip patch antenna with a rectangular radiation element has two fundamental resonances. The resonance at the lower frequency, i.e. the f_{10} frequency, corresponds to the length of the radiation element, while the resonance at the higher frequency, the f_{01} frequency, corresponds to its width. To construct a simultaneous shear and pressure sensor, we can place a U-shaped director above the radiation element of the microstrip patch antenna and separate these two component using a dielectric superstrate such as a layer of silicone prosthetic liner, as shown in Figure 1(c). Due to the EM coupling between the radiation element and the U-shaped director, the resonant frequencies of the patch antenna are influenced by the vertical distance between these two components as well as their lateral alignment. A pressure or shear force applied on the sensor package deforms the soft superstrate and thus changes the vertical and/or lateral positions of the U-shaped director. As a result, the antenna resonance frequencies shift correspondingly. Monitoring the two antenna resonant frequencies, therefore, enables deducing the applied pressure and shear forces simultaneously.

3. SENSOR DESIGN AND FABRICATION
The patch antenna was designed following conventional antenna design procedure (Tata et al. 2009). It was designed to have two fundamental frequencies of 6.1 GHz (TM_{010} mode) and 6.85 GHz (TM_{001} mode). As such, the radiation patch has a dimension of 12.75 mm in length and 11.25 mm in width for a substrate with a dielectric constant of a substrate with a dielectric constant of 3.5. The radiation element is fed by a 50 Ω microstrip transmission line at an inset location that matches the impedance of the radiation element to that of the transmission line (see Figure 2(a)). The U-shaped reflector was designed to have a total length of 26 mm and

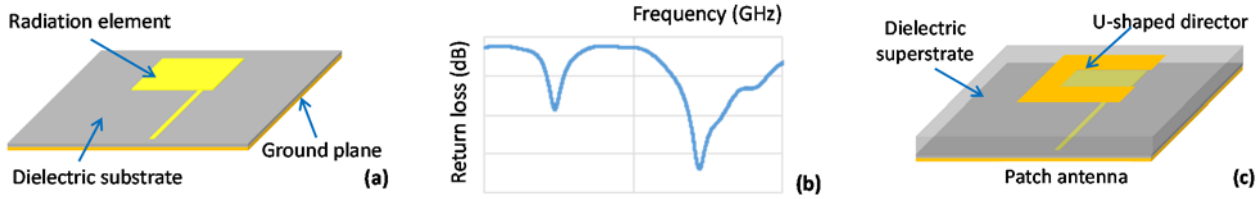

Figure 1. an antenna shear/pressure sensor; (a) microstrip patch antenna consisting of a ground plane, a rectangular radiation element, and a dielectric substrate; (b) typical S11 curve of a microstrip patch antenna with a rectangular radiation element. The antenna resonant frequencies are determined from the frequency positions of the local minima; (c) multi-layer microstrip patch antenna for shear and pressure sensing. The resonant frequencies of the microstrip patch antenna is dependent of the lateral and vertical position of the U-shaped director.

a width of 16.5 mm. The width of the slot is 5 mm and its length is 13 mm (see Figure 2(b)). The microstrip patch antenna and the U-shaped director were fabricated on a double-cladded printed circuit board using chemical etching technique. Initially, the antenna sensor was assembled into two sub-assemblies. The antenna sub-assembly was constructed by bonding the microstrip patch antenna on a mounting plate and then bonding a layer of liner material on top of the microstrip patch antenna, as shown in Figure 2(c). The U-shaped director bonded on a flat plate forms the director sub-assembly, as shown in Figure 2(d). Building these two sub-assemblies separately gives us more freedom in adjusting the lateral position of the U-shaped director during the sensor characterization process.

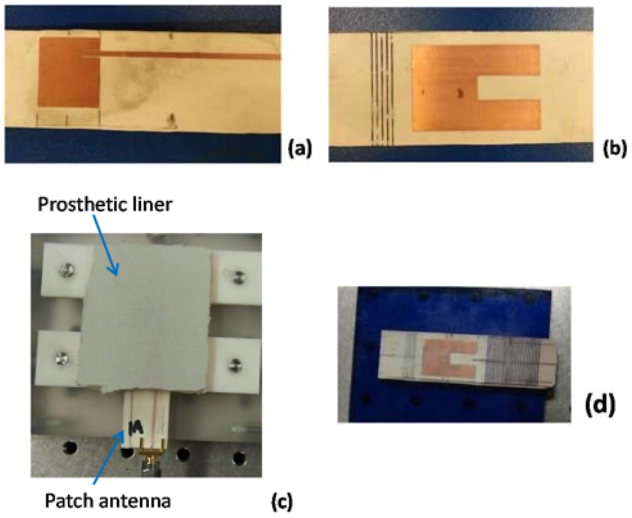

Figure 2. Implementation of antenna shear/pressure sensor; (a) microstrip patch antenna and (b) U-shaped director fabricated on conventional microwave circuit boards using chemical etching technique; (c) antenna sub-assembly constructed by bonding the patch antenna on a mounting plate and a layer of prosthetic liner glued on top of the radiation element; (d) director sub-assembly constructed by bonding the U-shaped director on a flat plate to facilitate shear application.

4. SENSOR CHARACTERIZATION

A test fixture that enables applying controlled shear and pressure displacements to the antenna sensor package were implemented and is shown in Figure 3. The sensor package is sandwiched between two plates; one is mounted under a load cell while the other one is mounted above an air bubble. Inflating the air bubble compresses the sensor package, which in turn pushes the upper plate against the load cell. The compression of the sensor package is measured using a linear variable differential transformer (LVDT) distance sensor mounted on the top plate. To apply shear pressure, a rod was screwed on the director plate and its position can be adjusted using a translation stage with a manual micrometer actuator. The displacement of the director plate was measured using an LVDT distance sensor mounted on the opposite side of the shear rod. The resonant frequencies of the microstrip patch antenna were measured by connecting the microstrip patch antenna to a vector network analyzer (VNA) using a coaxial cable. The S11 curve of the antenna sensor was measured under different combination of shear and pressure displacements. The shear displacement was applied first when the pressure was set to zero. Subsequently, pressure was applied incrementally by regulating the pressure of the bubble actuator.

The measured antenna resonant frequencies under different combinations of shear and pressure displacements are shown in Figure 4(a) and 4(b). The measurement data were curve fitted using second-order multivariate polynomials, i.e. $f = P_{00} + P_{10}*x + P_{01}*y$

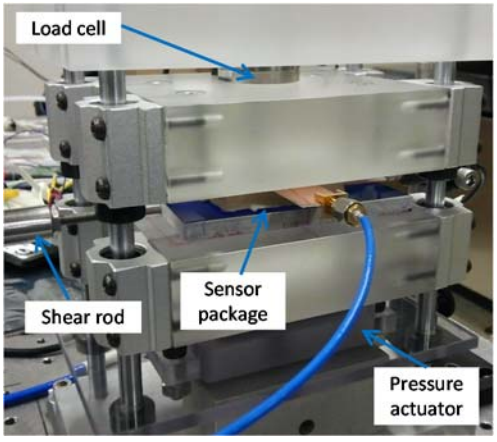

Figure 3. Test fixture for characterization of antenna shear/pressure sensor. Controlled pressure is applied to the sensor package using a bubble actuator while shear is applied manually using the shear rod. The pressure and shear displacements are measured using LVDT distance sensors.

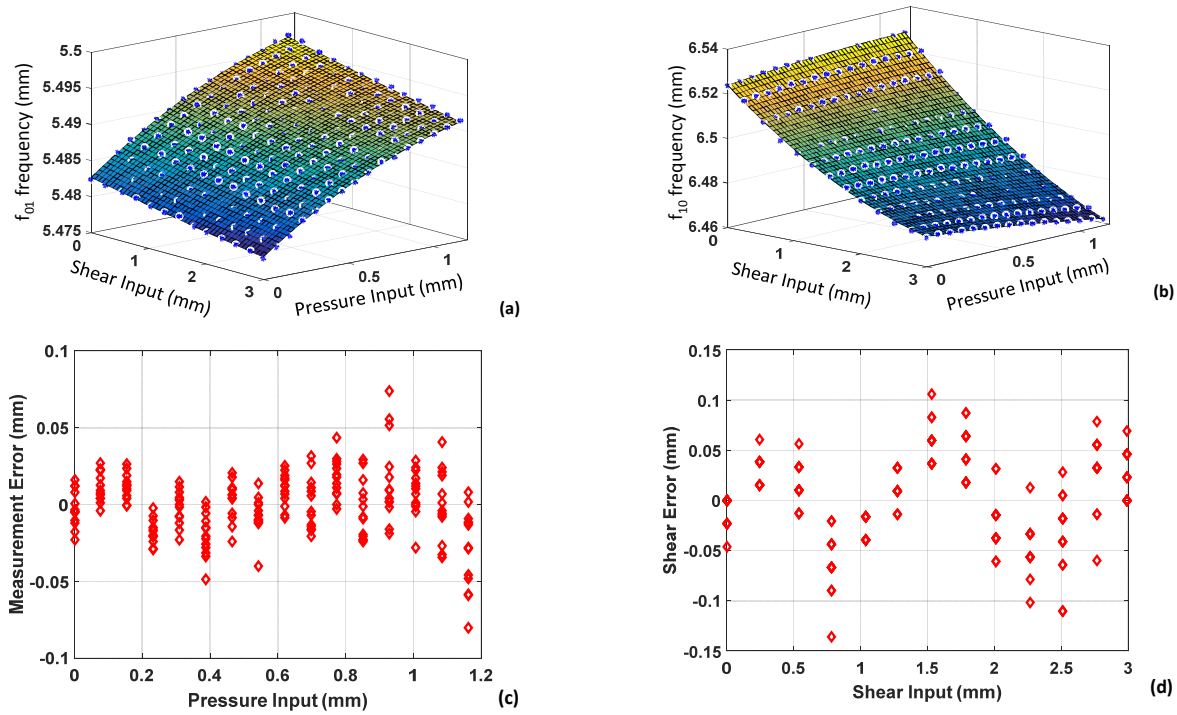

Figure 4. Validation of sensor performance; (a) & (b): the measured f_{01} and f_{10} frequencies fit using second-order multivariate polynomials; (c) & (d) differences between the pressure and shear displacements deduced from the measured antenna resonant frequencies and the displacements measured by the LVDT distance sensors.

$+ P_{20}*x^2 + P_{11}*x*y + P_{02}*y^2$. An R^2 value of 0.9979 was achieved for the f_{01} frequency while the R^2 value for the f_{10} frequency is 0.9980. Based on these fitting equations, an algorithm was developed to inversely calculate the shear and pressure displacements of the director plate from the measured antenna resonance frequencies. The differences between the shear and pressure displacements inversely determined from the measured antenna resonant frequencies and the actual shear and pressure inputs are shown in Figure 4(c) and 4(d). The total pressure displacement was 1.2 mm while the total shear displacement was 3 mm. The errors between the measured displacements and the actual inputs are within $\pm$0.1 mm for the pressure displacements and within $\pm$0.15 mm for the shear displacements, corresponding to $\pm$8% for the pressure and $\pm$5% for the shear displacements. Some of these errors may be contributed by the LVDT sensors, which have measurement uncertainties of around 0.06 mm.

5. COMPACT FMCW INTERROGATOR

In order to make the antenna sensor viable for prosthetic socket monitoring, a battery-powered portable interrogator was developed to replace the VNA. Since the amplitude of the signal reflected by the antenna sensor is frequency-dependent, we can detect the antenna resonance frequencies by supplying a frequency modulated continuous wave (FMCW) signal and measure the reflected power. The antenna resonance frequency can then be detected as the frequency at which the antenna reflects the least power. An FMCW signal generator was implemented by using a Voltage controlled Oscillator (VCO) controlled by a saw-tooth signal, as shown in Figure 5(a). A periodic saw-tooth signal is firstly generated using a 555 timer. The designed frequency of the output saw-tooth signal is 190 Hz and the voltage range is from 0.8 to 2.8 V. This signal is boosted to 3.1 V to 6.1 V using a voltage amplifier, which is then supplied to the VCO as the control signal to generate the periodic linear chip signal. Correspondingly, the VCO outputs a signal with a frequency sweeping from 1.7 to 2.3 GHz. Subsequently, a frequency multiplier chip triples the frequency of the VCO output. Thus, the interrogation frequency of the FMCW signal generator is increased to 5.1 to 6.9 GHz. In order to minimize the circuit size, the FMCW signal generator were implemented using surface mounted components. The circuit has two DC power voltages: 5 V and 12 V. The 5 V DC source provides the power for the 555 timer-based saw-tooth generator and the VCO. The 12 V powers the amplifier circuit. Both DC voltages are converted from a 3.7 V battery voltage using voltage regulator chips. The entire PCB FMCW transmitter can be powered by a 3.7 V lithium battery and the total power consumption of the circuit is around 160 mW.

The interrogation of the antenna sensor using the FMCW signal generator is shown in Figure 5(b). The FMCW signal is first filtered using a band pass filter to remove the harmonics and then is routed toward an antenna sensor using a circulator. The signal reflected by the antenna sensor is routed by the circulator to a power detector, which produces a direct-current (DC) signal that is inversely proportional to the input power. Finally, this DC signal is measured using a conventional data acquisition device, e.g. an oscilloscope. At current stage, discrete components are used for the band pass filter, the circulator, and the power detector. We will implement these components on a printed circuit board to reduce the size further. In addition, a data acquisition board with a fast sampling rate will be developed to replace the oscilloscope.

The DC outputs of the power detector were plotted versus time for one period of the saw-tooth signal, as shown in Figure 5(c). The antenna frequencies can then be detected from the two peaks of the power detector output. The shift of the antenna resonant frequencies with different director positions matched well with the S11 shifts shown in Figure 5(d) and thus confirms that we can use

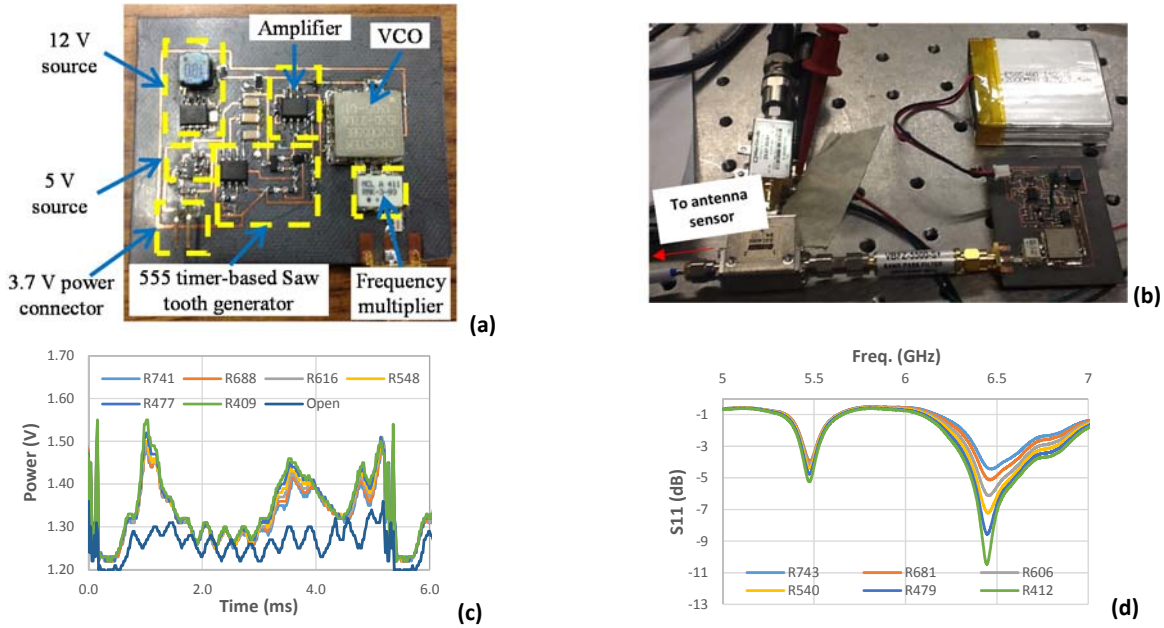

Figure 5. Validation of sensor performance; (a) & (b): the measured f_{01} and f_{10} frequencies fit using second-order multivariate polynomials; (c) & (d) differences between the pressure and shear displacements deduced from the measured antenna resonant frequencies and the displacements measured by the LVDT distance sensors.

the compact battery-powered interrogator to measure the antenna resonance frequencies.

6. CONCLUSION

A simultaneous shear and pressure sensor based on microstrip patch antenna technology was developed and characterized. By fitting the two fundamental frequencies of the microstrip patch antenna as second-order multivariate polynomials of the shear and pressure displacements, the shear and pressure displacements of the director can be inversely determined from the measured antenna resonant frequencies with an accuracy of ±8% for the pressure and ±5% for the shear displacements. A portable FMCW-based interrogator was also developed to facilitate the application of the shear/pressure sensor for prosthetic socket monitoring.

7. ACKNOWLEDGMENTS

This work was supported by the Office of the Assistant Secretary of Defense for Health Affairs, through the Peer Reviewed Orthopaedic Research Program under Award No. W81XWH-14-1-0502. Opinions, interpretations, conclusions and recommendations are those of the author and are not necessarily endorsed by the by the Department of Defense.

8. REFERENCES

[1]. Appoldt, F.A., Bennett, L. & Contini, R., 1970. Tangential pressure measurements in above-knee suction sockets. *Bulletin of Prosthetics Research*, 10(13), pp.70–86.

[2]. Mak, A.F.T., Zhang, M. & Boone, D.A., 2001. State-of-the-art research in lower-limb prosthetic biomechanics-socket interface: a review. *Journal of Rehabilitation Research and Development*, 38(2), pp.161–74.

[3]. Mak, A.F.T., Zhang, M. & Tam, E.W.C., 2010. Biomechanics of pressure ulcer in body tissues interacting with external forces during locomotion. *Annual Review of Biomedical Engineering*, 12, pp.29–53.

[4]. Meulenbelt, H.E.J. et al., 2006. Skin problems in lower limb amputees: a systematic review. *Disability and Rehabilitation*, 28(10), pp.603–8.

[5]. Meulenbelt, H.E.J. et al., 2011. Skin problems of the stump in lower limb amputees: 1. a clinical study. *Acta Dermato-venereologica*, 91(2), pp.173–7.

[6]. Sanders, J.E. et al., 2002. Interface pressure and shear stress changes with amputee weight loss - case studies from two trans-tibial amputee subjects. *Prosthetics and Orthotics International*, 26(3), pp.243–250.

[7]. Sanders, J.E., 2000. Thermal response of skin to cyclic pressure and pressure with shear: a technical note. *Journal of Rehabilitation Research and Development*, 37(5), pp.511–5.

[8]. Sanders, J.E., Daly, C.H. & Burgess, E.M., 1992. Interface shear stresses during ambulation with a below-knee prosthetic limb. *The Journal of Rehabilitation Research and Development*, 29(4), p.001.

[9]. Sundara-Rajan, K. et al., 2012. An interfacial stress sensor for biomechanical applications. *Measurement Science and Technology*, 23(8), p.085701.

[10]. Tata, U. et al., 2009. Exploiting a patch antenna for strain measurements. *Measurement Science and Technology*, 20(1), p.015201.

6th IEEE RAS/EMBS International Conference on
Biomedical Robotics and Biomechatronics (BioRob)
June 26-29, 2016. UTown, Singapore

Pneumatic Actuator Inserts for Interface Pressure Mapping and Fit Improvement in Lower Extremity Prosthetics

Wei Carrigan, Caleb Nothnagle, Prashant Savant, Fan Gao, Muthu B. J. Wijesundara, Senior m*ember, IEEE*

***Abstract*— The fit of a prosthetic socket to a residual limb is critical as poor socket fit is one of the leading causes of improper function, discomfort, and skin breakdown. The daily and long term volume fluctuation of a residual limb presents a major challenge to maintaining fit. This work presents the initial efforts to develop adjustable inserts that consisted of arrays of small, sensorized inflatable pressure actuators that can expand based on the volume change. We have fabricated and tested actuator inserts to demonstrate their capability for pressure mapping in a limb-socket interface. We have also shown that the actuators have the capacity to maintain positive displacement under load to accommodate for volume change in a residual limb for improved fit.**

I. Introduction

The fit of a prosthetic socket to a residual limb is critical for proper load transmission, stability, and control over mobility. Poor socket fit is one of the leading causes of improper function, discomfort, skin breakdown, and limb abandonment. Sockets are designed and fit such that loads are mainly placed upon load bearing areas while mitigating the loads on sensitive areas. Proper fit of a socket can be evaluated by studying the dynamic pressure variation at each load bearing area during the gait cycle. The average pressure variation of these load bearing areas can vary widely from 20 to 120kPa [1, 2]. Regardless of how well the socket is initially fit to the amputee, daily and long term volume fluctuation in the residual limb presents a major challenge to practitioners and wearers [3]. Although many approaches have been proposed and used to correct the effect of volume fluctuation, it remains one of the leading causes of amputees abandoning their prosthesis [4].

There are many techniques used to accommodate for residual limb volume and shape changes, all of which have limitations. One key problem is the non-uniform nature of the limb's volume and shape changes through diurnal and long term. For example, adding/removing socks of different thicknesses modulates the thickness uniformly but does not restore the interface pressure to its original level because volume changes are not uniform throughout the residual limb [5]. Though inflatable air-bladders could offer variable stiffness and sizes, they compress excessively during walking and are unable to maintain uniform and consistent support to the residual limb [6]. A recently developed socket manually loosens/tightens predetermined load bearing areas, yet all are adjusted equally which may result in undesired pressures in some regions as the volume and shape of the limb changes [www.clickmedical.co]. Though all of these current strategies provide some assistance in overcoming prosthetic fit issues, the ideal interface should be an adaptive device that can accommodate the amount of volume change in specific areas of the residual limb. Making a device that can identify the level of adjustment needed at a given area of the limb and can address each area individually is challenging [7].

The work presented here describes an initial step towards realizing an adaptive interface that can determine and adjust the pressure level required at given areas to accommodate for uneven volume change in the residual limb. For this, we are using inserts that consist of arrays of small, sensorized inflatable pressure actuators that can expand based on the volume change at targeted areas to improve the fit. The initial work is to use these small segmented actuators at load tolerant areas of the residual limb. We will investigate the initial design of the actuator for load bearing and volume change capability. Further, we will discuss the interface pressure and actuator response during simulated walking in two load tolerant areas, i.e. medial and anterior by incorporating the actuators to a modified socket. These results will allow us to improve the actuator design and actuation pressure modulation scheme for a better prosthetic fit.

II. Actuator Design and Test System Description

A. Actuator Design and Fabrication Process

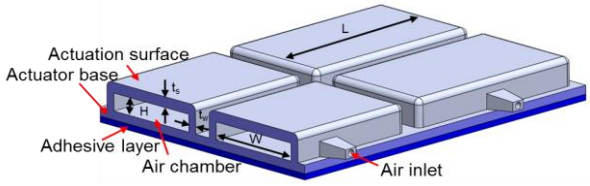

Figure 1. Schematic drawing of an actuator patch.

*Research supported by the Office of the Assistant Secretary of Defense for Health Affairs through the Peer Reviewed Orthopedic Research Program under Award No. W81WXWH-14-1-0502. Opinions, interpretations, conclusions and recommendations are those of the author and are not necessarily endorsed by the Department of Defense.

W. Carrigan is with the University of Texas at Arlington Research Institute, Fort Worth, TX76118 USA (e-mail: kcarrigan@uta.edu).

C. Nothnagle is with the University of Texas at Arlington Research Institute, Fort Worth, TX76118 USA (e-mail: calebn@uta.edu).

F. Gao is with University of Texas Southwestern Medical Center, Dallas, TX 75390, USA (e-mail: fan.gao@utsouthwestern.edu)

P. Savant is with the University of Texas at Arlington Research Institute, Fort Worth, TX76118 USA (e-mail: prashant@uta.edu).

M. B. J. Wijesundara is with the University of Texas at Arlington Research Institute, Fort Worth, TX76118 USA, (corresponding author to provide phone: 817-2720-5994; fax: 817-272-5952; e-mail: muthuw@uta.edu).

A single pneumatic actuator insert consists of several small bubble actuators which can be inflated/deflated individually or in groups. The generic shape of all actuators is an air chamber with an approximate size of 30mm(L)×20mm(W)×3mm(H). The side wall thickness is 1mm (t_w) and the top surface actuation membrane thickness (t_s) is 1.75mm. The overall base thickness is about 2mm. These values are selected based on simulation results (not reported here) to satisfy the desired expansion displacement. Fig. 1 shows the generic configuration of the actuator insert.

The actuator insert is fabricated using a combination of compression and over-molding techniques. All molds were 3D printed within an accuracy of 100µm and were coated with a thin layer of Parylene C (Special Coating System™) film for demolding purposes. All actuator inserts are fabricated using RTV silicone rubber (XIAMETER® RTV-4234-T4, Xiameter ®, Dow Corning).

The top part of the actuator is fabricated through a compression molding technique by mating a positive mold (Fig. 2(a)) with a negative mold filled with the liquid form of elastomeric material (Fig. 2(b)) as shown in Fig. 2. Small pins are inserted into the mated molds for removing the material to form the air channels (Fig. 2(c)). After thermosetting, the top part of the actuator comprising of air chambers is removed from the molds (Fig. 2(d)). By placing the top part of the actuator onto a base mold filled with a known amount of liquid elastomeric material, the actuator base with a defined thickness is bonded to the top part to form a sealed air chamber (Fig. 2(e) and (f)).

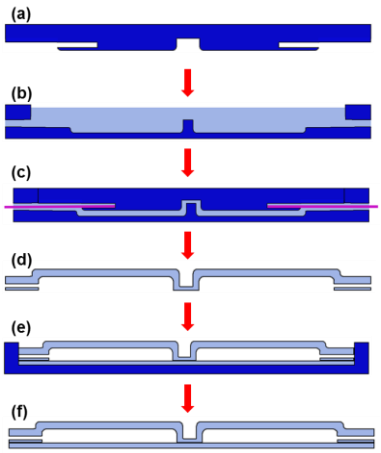

Figure 2. Fabrication process of the actuator insert; (a) a positive mold (top mold); (b) negative mold (bottom mold) filled with liquid elastomer; (c) assembled top and bottom molds with inserted pins; (d) top part of actuator after thermosetting; (e) top part of actuator sitting on prefilled liquid elastomer; (f) actuator insert after thermosetting.

B. *Limb-socket System Description*

The limb-socket system used to investigate actuator insert response during simulated walking is shown in Fig. 3. This system comprises of a modified prosthetic socket with an attached pylon and foot, actuator inserts, and a fabricated stump covered with a sensorized liner. A prosthetic socket, Fig. 3(a), made of thermoplastic with recessed pockets at load tolerant areas to accommodate for actuator inserts is fabricated by the Prosthetic and Orthotics Lab at UT Southwestern Medical Center using a residual limb model. Airline ports are created at the recessed pockets to route pneumatic tubing outside of the socket, avoiding interference with the pressure interface and providing a means of actuation to the inserts. These actuator inserts, Fig. 3(b), are fabricated to match load tolerant areas including patellar ligament, anterior compartment, medial tibial flare, medial shaft of tibia, lateral shaft of fibula, and posterior compartment [8]. Fig. 3(c) shows their placement within the modified prosthetic socket. The fabricated stump, molded to match a residual limb as seen in Fig. 3(d), is created using Plaster of Paris and is covered with a sensorized liner. This liner has interface pressure sensor array patches fixed at the medial (medial tibial flare and medial shaft of tibia) and anterior (anterior compartment) locations for this study. Fig. 3(e) shows the complete prosthetic interface test socket with integrated actuator inserts and associated external airlines. Fig. 4 illustrates the details of the limb-socket interface with embedded actuator inserts.

Additionally, pneumatic and sensing hardware is included to conduct testing. Fig. 5 shows the major components for actuation and sensing of the actuator inserts. An air supply (not shown in figure), comprising of a pump and air pressure regulator, is distributed to the inserts through a solenoid manifold which allows for control over each individual actuator's pressurization. The solenoids are toggled by a switchboard of MOSFETs connected to a microcontroller which takes input from a Matlab graphical user interface (GUI). The internal pressure of the actuators is monitored by an array of air pressure sensors whose output is read by a secondary microcontroller and recorded through the GUI. A F-Socket system (Tekscan, Inc.) is used to map the interface pressure through an array of sensor elements and outputs to a dedicated data acquisition module.

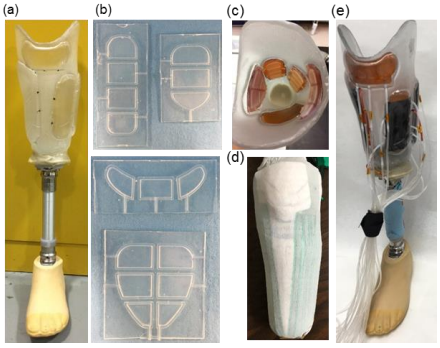

Figure 3. (a) Demonstration of a fabricated socket with recessed pockets at load tolerant areas; (b) example actuator inserts in different shapes; (c) close-up view of actuator patches embedded in the recessed pockets before actuation; (d) fabricated stump with sensorized liner; (e) modified socket with embedded actuator inserts and connected pneumatic tubing.

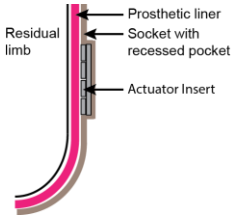

Figure 4. Illustration of limb-actuator insert-socket interface with embedded actuator insert.

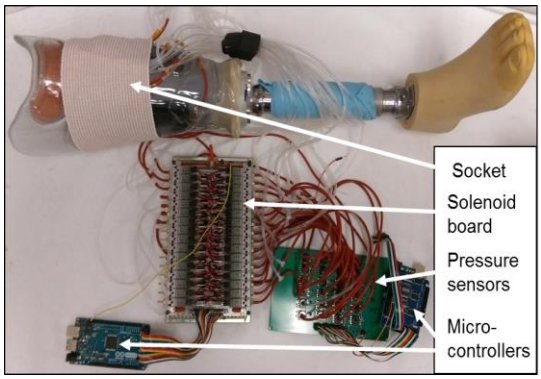

Figure 5. Pneumatic and sensing hardware.

III. EXPERIMENTAL

A. Actuator Characterization

The actuator insert experiences expansion and compression during all phases of its use and most importantly during prosthetic fitting adjustment. The actuator insert not only accommodates for residual volume fluctuations but also bears the load at the interface. Actuator characterization is performed to obtain a baseline curve of the positive displacement at different actuation pressures to exam whether it can satisfy the residual limb volume change in the radial direction. A correlation between actuator displacement and internal pressure variations under loading conditions will help to define the actuator status when it is placed at the interface. This will also help determine the required initial actuation pressure to maintain a positive displacement of the insert while under loading at the interface.

The setup used to carry out the experimental evaluation is shown in Fig. 6. For the displacement measurement, the position of the loading plate is controlled along all axes and is initially placed at the same level as the unactuated membrane surface. Once the actuator is inflated at a constant pressure, the loading plate is slowly moved up until it no longer contacts the membrane surface. Then the loading plate is slowly moved back to contact the membrane surface without affecting the initial pressure value. The measured distance of the loading plate from the initial membrane level is the positive displacement of the actuator at the set inflation pressure. This test is performed with three actuators using actuation pressures ranging from 0 to 41kPa.

As aforementioned, the actuator should also be able to bear the external force of a residual limb while standing or walking. This load bearing capability test is performed with a similar setup and procedure as when measuring the positive displacement of an actuator; however, the loading plate is free to move in the z axis and has a known weight placed on it as shown in Fig. 6. The actuator is inflated to an initial pressure which is then closed to the air supply by closing a valve to the pressure regulator. A pressure sensor will then read the internal pressure changes of the actuator as an incremental load is applied and a displacement indicator will read the corresponding displacement in the z axis. The actuator displacement change during this test is illustrated in Fig. 7. The recorded data will provide the relationships between applied external force, displacement, and internal pressure variation. This test is performed with two initial actuation pressures, 27 and 41kPa.

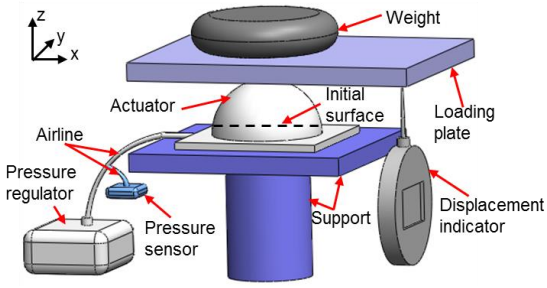

Figure 6. Schematic test setup for actuator characterization.

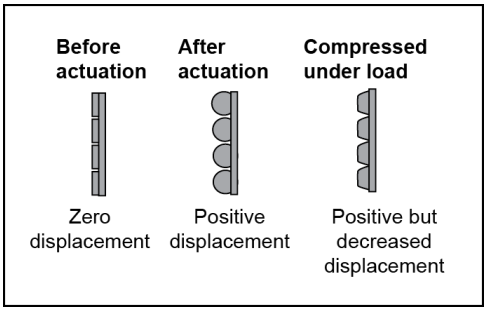

Figure 7. Illustration of displacement changes at different stages.

B. Limb-socket Test Setup

To investigate the actuator insert's performance during a walking motion, a gait simulation, similar to the roll over method used in prosthetic feet analysis, is performed [9]. By continuously mapping the interface pressure and recording the corresponding internal pressure of the actuator inserts at the anterior and medial locations of a residual limb, the load bearing capabilities of the actuator inserts within a prosthetic socket will be assessed.

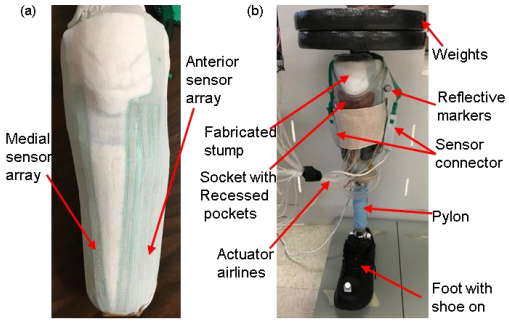

Figure 8. (a) The fabricated stump covered with sensorized liner; (b) setup used in limb-socket test.

A fabricated stump covered with a sensorized liner is inserted into a prosthetic socket with embedded actuator inserts. The inserts are actuated with an internal pressure of 27kPa after which a 45.5kg weight is added onto the fabricated stump to simulate body weight. The stump is actively rolled forward and backwards at angles of ±30° from a normal, upright position (mid-stance) so as to imitate the toe-off and heel-strike motions. This motion is repeated over a 100s test period with the stump being held in the forward and backward positions for 5 second intervals. A fitted shoe is worn by the foot to ensure solid ground contact. Four

reflective markers are placed at two sides of the ankle and knee to track the knee trajectory while two markers placed in the front and back of the shoe track the location of the toe and heel relative to the ground, as seen in Fig. 8.

IV. Results and Discussion

A. Actuator Characteristic

The actuator inserts are meant to accommodate the residual volume fluctuation and bear the load at the residual limb-socket interface. A first set of tests was performed to identify the expansion displacement characteristics of the current actuator design. Fig. 9 represents the expansion displacement data for three actuators when inflated to pressures ranging from 0kPa to 41.4kPa. These data show that actuators expand up to 6.4±0.39mm at the highest tested actuation pressure. A previous report shows that the typical residual limb volume change in the radial direction can change as much as ±2.55mm [10]; therefore, the current actuator design has the capacity to accommodate for residual limb volume fluctuations.

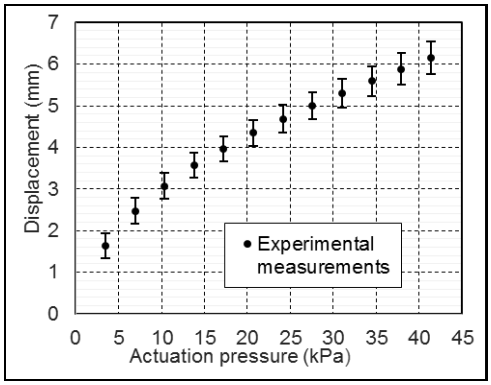

Figure 9. Measured positive displacement at different actuation pressure.

A key aspect of the actuator is that it should bear the external force from the residual limb while standing or walking and maintain positive displacement values. We simultaneously tracked the displacement and internal pressure variation of the actuator subjected to external force. Applied external forces compress the actuator which reduces its total displacement while increasing its internal pressure.

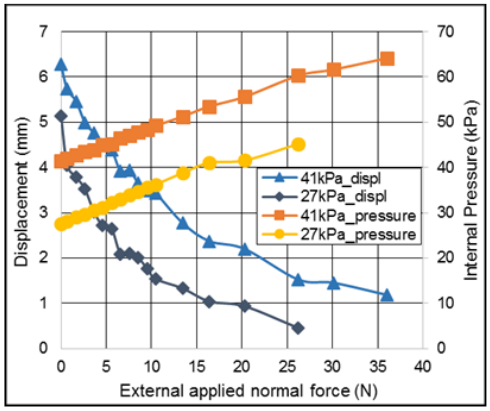

Figure 10. The decrease in displacement and increase in internal pressure of an actuator when increasing the applied external force from 0 to 36N with an initial actuation pressure of 27 and 41kPa.

Fig. 10 shows the decrease in total displacement and increase in internal pressure of a single actuator when an external force, ranging from 0 to 36N, is applied to an actuator with a baseline actuation pressure of 27 and 41kPa. An actuator with an initial positive displacement of 5mm and internal pressure of 27kPa will shrink down to 0.5 mm at 27N of applied external force. The corresponding internal pressure increases to 46kPa; therefore, to maintain positive actuator displacement, an actuator inflated at 27kPa should not experience internal pressures over 46kPa during operation. Based on data for actuators with an initial pressure of 41kPa, these actuators retain a certain amount of positive displacement even at external loads exceeding 36N. These data clearly indicate that the internal pressure variation can be used as a reference to determine the positive displacement and needed actuator inflation pressure to prevent collapsing at different loading conditions.

B. Limb-socket Performance with Actuator Inserts

The internal pressure variation of an actuator indicates its behavior during simulated walking while its effect on the fabricated limb is reflected by the mapped interface pressure. Though actuator inserts are located across all five load bearing areas, this investigation was limited to the anterior and medial (medial tibial flare and medial shaft of tibia) sections of the fabricated stump. Upon inserting the limb into the socket and inflating the actuator inserts at 27kPa, no measurable pressure readings were observed by the interface pressure sensors which ensures the actuators' positive displacement has reached their expected value according to Fig. 10. At this point, a 45.5kg weight was placed on the fabricated limb as seen in Fig. 8(b) and the simulated walking motion was performed.

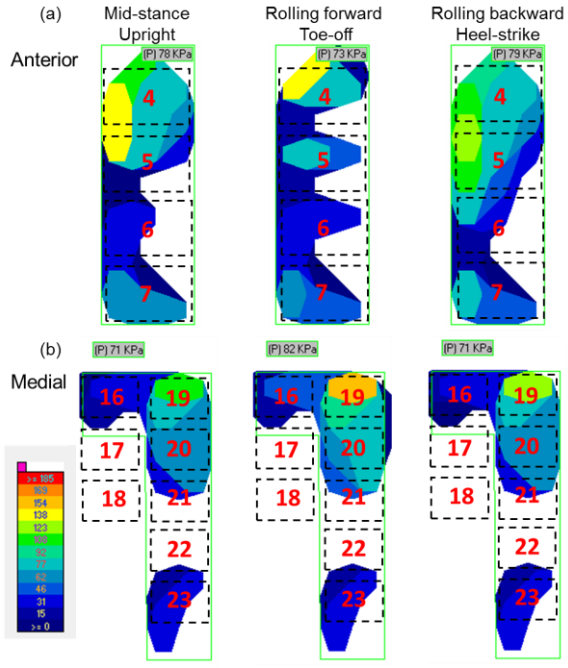

Figure 11. "Average" contact pressure mapped at mid standace (upright) postion, rolling forward (toe-off) position, and rolling backward (heel-strike) position for (a) anterior and (b) medial areas.

Fig. 11 shows the interface pressure profile at the medial and anterior areas at three positions with an overlay

indicating the location of the actuator inserts. At an upright position, the pressure profile indicates uneven distribution which can be seen throughout previously reported data on different socket interfaces [11]. During the forward motion, the peak interface pressure occurs at the proximal area for both anterior and medial locations. When moved backwards, the peak pressure for the anterior location translated downward and the contact pressure distributed more evenly. In the medial location, the forward position resulted in an increase in peak pressure in the proximal area while the backwards position reduced the magnitude of this pressure; however, no significant change in contact pressure distribution was observed. The reported trends of pressure variation at these locations during the gait cycle are in agreement with this presented data [11, 12].

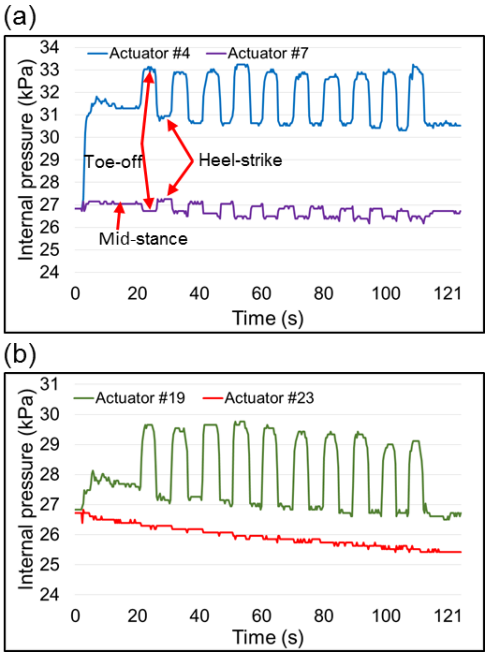

Figure 12. Internal pressure variation of (a) actuator 4 and 7 for anterior and (b) actuator 19 and 23 for medial.

While conducting this test, the internal pressure of each actuator insert was recorded to examine the actuator behavior under loading. Fig. 12 represents the internal pressure variation data of the actuators with an initial inflation pressure of 27kPa at selected locations which correspond to actuators 4 and 7 for the anterior and 19 and 23 for the medial. Actuators 4 and 19 are focused on as they experienced the highest interface peak pressure throughout the test (see Fig. 11). In the anterior location, actuators 4 and 7 observed opposite behavior; i.e. the internal pressure experienced by actuator 4 decreases from the toe-off to heel-strike positions while the interface pressure of actuator 7 shows an increase. In the medial location, actuator 19 observed a decrease in internal pressure from toe-off to heel-strike whereas actuator 23 experienced no significant change.

Based on the highest internal pressure experienced during motion, 33kPa in the anterior actuator 4 and 29.7kPa for the medial actuator 23, the actuator insert's internal pressure in this limb-socket test are below the load bearing threshold of their design according to Fig. 10. Therefore, these inserts can withstand the load of a 45.5kg weight and maintain positive displacement to accommodate for volume changes in a residual limb.

When correlating the interface pressure data to the internal pressure variations, a trend clearly exists between corresponding actuators. Both interface and internal actuator pressure increase at the toe-off position and decrease at the heel-strike position for actuators 4 and 19. On the other hand, both interface and internal actuator pressure decrease at the toe-off position and increase at the heel-strike position for actuator 7. No significant changes were observed for either interface or internal actuator pressure at actuator 23. Therefore, these data support a correlation between the internal pressures of actuators to their interface pressures at the limb-socket interface suggesting that internal pressure of actuators can be used in an effort to distribute interface pressure for a better prosthetic fit.

V. Conclusion

We have successfully fabricated and tested actuator inserts that can be used in a modified prosthetic socket to improve fit. With these initial studies on small segmented actuator inserts, we have demonstrated their capability to map the pressure at a limb-socket interface. Though these actuators' internal pressures are not direct measurements of interface pressure, the internal pressure of the actuators can be used to derive the interface pressure and modulate it so as to achieve a better prosthetic fit.

VI. Future Work

To further investigate the applicability of actuator inserts to accommodate volume fluctuation in the residual limb while maintaining fit, we plan to use residual limbs with slight volume variation as well as human subjects to evaluate the performance of the actuators. It is understood that the current actuator system may experience reduced contact surface area when accommodating for a large displacement in the residual limb. This will be addressed by variations in the membrane design such as membrane thickness along the side walls and corrugated wall membranes to improve the contact area. Other planned experiments include investigation of gait patterns at different inflation parameters so that proper gait characteristics may be maintained.

The current control system has been designed for concept validation in a laboratory setting; however, future efforts will include steps to miniaturize the control setup and improve its response to dynamic loading. The goal of miniaturization will be to reduce the size and weight of the system down to a wearable device which may be carried by the user in either a satchel or small waist pack. Due to the relatively small volume of the actuators, the response time of the system can be improved. This will allow the system to respond to dynamic changes during the gait cycle.

Acknowledgment

This work was supported by the Office of the Assistant Secretary of Defense for Health Affairs through the Peer

Reviewed Orthopedic Research Program under Award No. W81WXWH-14-1-0502. Opinions, interpretations, conclusions and recommendations are those of the author and are not necessarily endorsed by the Department of Defense.

The authors would like to extend their thanks the staff of UTARI and the Prosthetic and Orthotics Lab at UT Southwestern for their contributions as well as the following individuals: Mahdi Haghshenas-Jaryani, Ryan Landrith, and Charu Pande.

REFERENCES

[1] T. Dumbleton, A. W. P. Buis, A. McFadyen, B. F. McHugh, G. McKay, K. D. Murray, and S. Sexton, "Dynamic interface pressure distributions of two transtibial prosthetic socket concepts," Journal of Rehabilitation Research and Development, vol. 46, no. 3, pp. 405-416, 2009.

[2] T. L. Beil, G. M. Street, and S. J. Covey, "Interface pressures during ambulation using suction and vacuum-assisted prosthetic sockets," Journal of Rehabilitation Research and Development, vol. 39, no. 6, pp. 693-700, 2002.

[3] J. E. Sanders and S. Fatone, "Residual limb volume change: systematic review of measurement and management," Journal of Rehabilitation Research and Development, vol. 48, no. 8, pp. 946-986, 2011.

[4] P. Sewell, S. Noroozi, J. Vinney, and S. Andrews, "Developments in the trans-tibial prosthetic socket fitting process: A review of past and present research", Prosthetics and Orthotics International, vol. 24, no. 2, pp. 97–107, 2000.

[5] J. E. Sanders, J. R. Fergason, S. G. Zachariah, and A. K. Jacobsen. "Interface pressure and shear stress changes with amputee weight loss - case studies from two trans-tibial amputee subjects", Prosthetics and Orthotics International, vol.26, no. 3, pp. 243-250, 2002.

[6] J. E. Sanders and D. V. Cassisi, "Mechanical performance of inflatable inserts used in limb prosthetics", Journal of Rehabilitation Research and Development, vol. 38, no. 4, pp. 365–74, 2001.

[7] R. M. Greenwald, R. C. Dean, and W. J. Board, "Volume Management : Smart Variable Geometry Socket (SVGS) Technology for Low-limb Prostheses", American Academy of Orthotists and Prosthetists, vol. 15, no. 3, pp. 107–112, 2003.

[8] S. Kapp and D. Cummings, "Transtibial amputation: Prosthetic management", Chapter 18B, Atlas of Limb Prosthetics: Surgical, Prosthetic, and Rehabilitation Principles. Rosemont, IL, American Academy of Orthopedic Surgeons, edition 2, 1992, reprinted 2002.

[9] C. Curtze, A. L. Hof, H. G. van Keeken, J. P. Halbertsma, K. Postema, and B. Otten, "Comparative roll-over analysis of prosthetic feet", J Biomech, vol. 42. No. 11, pp. 1746-1753, 2009.

[10] S. G. Zachariah, R. Saxena, J. R. Fergason, and J. E. Sanders, "Shape and volume change in the transtibial residuum over the short term: Preliminary investigation of six subjects," Journal of Rehabilitation Research and Development, vol. 41. No. 5, pp. 683-694, 2004.

[11] P. Convery and A. W. P. Buis, "Socket/stump interface dynamic pressure distributions recorded during the prosthetic stance phase of gait of a trans-tibia1 amputee wearing a hydrocast socket", Prosthetics and Orthotics International, vol. 23, pp. 107-112, 1999.

[12] P. Convery and A. W. P. Buis, "Conventional patellar-tendon-bearing (PTB) socket/stump interface dynamic pressure distributions recorded during the prosthetic stance phase of gait of a trans-tibial amputee", Prosthetics and Orthotics International, vol. 22, pp. 193-198, 1998.